Physical and biogeochemical controls over terrestrial ecosystem responses to nitrogen deposition

GREGORY P. ASNER[1]*, ALAN R. TOWNSEND[2], WILLIAM J. RILEY[3],
PAMELA A. MATSON[4], JASON C. NEFF[5] & CORY C. CLEVELAND[2]
[1]*Department of Geological Sciences and Environmental Studies Program, University of
Colorado, Boulder, CO 80309 U.S.A.;* [2]*Department of EPO Biology and INSTAAR,
University of Colorado, Boulder, CO 80309 U.S.A.;* [3]*Department of Civil and Environmental
Engineering, University of California, Berkeley, CA 94720 U.S.A.;* [4]*Department of
Geological and Environmental Sciences, Stanford University, Stanford, CA 94305 U.S.A.;*
[5]*Natural Resource Ecology Laboratory, Colorado State University, Ft. Collins, CO 80523
U.S.A. (*Author for correspondence)*

Abstract. Anthropogenic perturbations to the global nitrogen (N) cycle now exceed those to
any other major biogeochemical cycle on Earth, yet our ability to predict how ecosystems
will respond to the rapidly changing N cycle is still poor. While northern temperate forest
ecosystems have seen the greatest changes in N inputs from the atmosphere, other biomes,
notably semi-arid and tropical regions of the globe, are now experiencing increases in N
deposition. These systems are even less well understood than temperate forests, and are likely
to respond to excess N in markedly different ways. Here, we present a new integrated terrestrial
biophysics-biogeochemical process model, TerraFlux, and use this model to test the relative
importance of factors that may strongly influence the productivity response of both humid
tropical and semi-arid systems to anthropogenic N deposition. These include hydrological
losses of dissolved inorganic and organic N, as well as multiple nutrient interactions with
deposited inorganic N along the hydrological pathway. Our results suggest that N-rich trop-
ical forests may have reduced productivity following excess N deposition. Our simulations
of semi-arid systems show increases in productivity following N inputs if water availability
is sufficient and water losses are moderate. The most important model controls over the
carbon cycle response in each simulation were interactions that are not represented in the
most common terrestrial ecosystem models. These include parameters that control soil solute
transport and nutrient resorption by plants. Rather than attempt prognostic simulations, we use
TerraFlux to highlight a variety of ecological and biogeochemical processes that are poorly
understood but which appear central to understanding ecosystem response to excess N.

Introduction

Agricultural and industrial intensification in recent decades have led to dramatic increases in the production of airborne reactive nitrogen (N) (Logan 1985; Smil 1990; Galloway et al. 1995; Vitousek et al. 1997). Today, atmospheric concentrations of both oxidized (NO_y) and reduced (NH_x) reactive nitrogen compounds vary strongly by region (Chameides et al. 1994), but are highest in locations around and downwind from major source areas such as the northeast U.S., western and central Europe, and east Asia (Holland et al. 1999). This excess atmospheric N, in turn, leads to higher N deposition to both terrestrial and aquatic ecosystems. Some temperate latitude regions have now experienced chronically elevated inputs of N for decades (Berendse et al. 1993, Wright & Van Breemen 1995; Fenn et al. 1998), and such inputs are projected to continue increasing in the future (Galloway et al. 1994).

Many studies have highlighted the potentially deleterious effects of anthropogenic N deposition in ecosystems (e.g., Agren & Bosatta 1988; Aber et al. 1989; Howarth et al. 1996; Magill et al. 1997; Asner et al. 1997; Tietema et al. 1997; Currie & Nadelhoffer 1999; Matson et al. 1999; Nadelhoffer et al. 1999). Theories introduced by Agren & Bosatta (1988) and Aber et al. (1989) suggested that N deposition would initially stimulate net primary productivity (NPP) in terrestrial ecosystems of the temperate latitudes, where deposition rates were (and continue to be) highest and where N limits plant productivity (Vitousek & Howarth 1991). These theories also predicted that N deposited in temperate ecosystems could eventually lead to N saturation. The N saturation concept has been defined in a variety of ways (e.g., Agren & Bosatta 1988; Aber et al. 1989; Binkley & Hogberg 1997), but it generally refers to an increase in nitrate mobility in soils, an increase in N losses from an ecosystem, and potential decreases in N-stimulated plant growth.

While temperate forest ecosystems have unquestionably experienced the greatest increases in N inputs from the atmosphere, global patterns of N deposition have changed only in the last decade (e.g., Holland et al. 1999). In the past few years, the most dramatic increases in N deposition have been in systems that are very different from temperate forests, such as many regions of the tropics, where rates of population and industrial growth are most rapid (Matson et al. 1999). Future projections of N deposition suggest that these regions will continue to see marked increases in N inputs (Galloway et al. 1994). Although plant productivity in most temperate forest ecosystems is constrained by nitrogen availability (Vitousek & Howarth 1991), evidence suggests that humid tropical systems often cycle N in relative excess, and that plant growth is limited by other resources (Vitousek 1982; Vitousek & Sanford 1986; Martinelli et al. 1999). Matson et al. (1999) point out that this excess of N in tropical systems might pre-dispose these regions to more rapid

and negative responses to increased N deposition. They suggest that excess N may lead to rapid increases in emissions of N-containing trace gases, a hypothesis supported by fertilizer experiments in Hawaii (Hall & Matson 1999).

Matson et al. (1999) also suggest that excess N inputs will lead to higher rates of nitrate leaching, and that such losses could drive losses of elements that may already limit plant growth. Mobile NO_3^- can capture and transport Ca^{2+}, Mg^{2+}, and other cations, as has been observed in N-limited (now potentially N saturated) temperate ecosystems (Likens et al. 1996; Emmett et al. 1995; Currie et al. 1996). Aber et al. (1989) suggested that excessive rates of N deposition, such as those observed in the northeastern U.S. and Europe, could also lead to decreases in plant productivity through indirect processes such as soil acidification and base cation impoverishment. Under similar conditions, there is a risk of mobilizing base cations in tropical soils, which for the most part, are already in poor supply in many lowland tropical systems (e.g., Vitousek 1982; Cuevas & Medina 1988). Cation impoverishment could therefore result in significant changes to the carbon cycle of the humid tropics.

Recent work also indicates that NH_x and NO_y deposition is increasing in arid and semi-arid regions of the world. Holland et al. (1999) show that NO_y deposition reaches 10 kg ha^{-1} yr^{-1} in western U.S. ecosystems, and that NH_x deposition can exceed 10 kg ha^{-1} yr^{-1} in savanna-grasslands of northern Argentina and southern Brazil. In contrast to humid tropical forests, productivity in arid and semi-arid ecosystems is considered to be water and N limited (e.g., Romney et al. 1978; Medina & Silva 1990; McLendon & Redente 1992). An increase in N deposition here could stimulate plant growth, but the seasonally episodic rainfall patterns could also lead to significant losses of any added N.

Water infiltration tends to be higher in grasslands and on sandier soils than it is in shrublands and on clayey soils, where lateral runoff dominates (Bach et al. 1986; Abrahams et al. 1995). Therefore, differences in vegetation cover and soil physical (and chemical) properties affect the vertical and lateral flow partitioning of biologically important forms of N, P and cations in these systems (e.g., Nishita & Haug 1973; Lajtha & Bloomer 1988; Schlesinger et al. 1999, 2000). For example, Schlesinger et al. (1999) showed significant lateral losses of N in dissolved organic and inorganic forms following simulated rainfall events in an arid shrubland. The processes controlling these lateral water fluxes in shrubland ecosystems, such as infiltration rate, micro-topography and vegetation patchiness, would presumably exert control over the potential fertilization effect of atmospheric N deposition in these ecosystems. Observed variations in the depth of the $CaCO_3$ deposits in arid

ecosystem soils support the notion that vertical water (and thus N) transport is significant yet varies markedly based on soil physical and chemical properties (Arkley 1963). The fate of excess N could also be different in the grass-lands and savannas, where greater infiltration and less evaporative loss could favor vertical transport over lateral runoff. The semi-arid Brazilian cerrado savanna, Argentina's Pampas grassland, and the U.S. Great Plains grassland are relatively productive with higher vegetation cover than in arid shrublands (Defries et al. 1995). All of these regions undergo strong atmospheric convec-tion, resulting in a rainfall regime that is highly episodic in both space and time (O'Connor 1994). A potential fertilizing effect of increased N deposition will therefore depend strongly upon the hydrological transport characteristics of soils in these regions.

Several research efforts have focused on NPP and C sequestration responses that could occur in ecosystems resulting from N deposition (Peterson & Melillo 1985; Schindler & Bayley 1993; Hudson et al. 1994; Townsend et al. 1996; Holland et al. 1997). However, recent experimental studies have shown that traditional assumptions about how N inputs might affect plant growth may be flawed. Long-term fertilization studies combined with isotopic labeling in both eastern U.S. and European forests show the bulk of added N has not entered the vegetation, and therefore has not stimulated significant C uptake (Magill et al. 1997; Tietema et al. 1997; Nadelhoffer et al. 1999; Currie & Nadelhoffer 1999). Rather, most of the recently added N presently appears to be in surface soil horizons, with yet unknown mechan-isms and time-scales of turnover (Aber et al. 1998; Nadelhoffer et al. 1999). While such fertilization studies cannot unquestionably demonstrate how a system may respond to much longer-term, chronic N inputs, they do suggest that unlike earlier assumptions, excess N inputs to N-limited forests may not cause strong and rapid new C storage. These studies emphasize the difficulty in predicting the effects of N deposition in temperate forests, despite the fact that these systems are better studied that most others on Earth.

Both the biogeochemical and hydrological regimes of humid tropical and semi-arid ecosystems are sufficiently different from temperate forests to cause even greater uncertainty in the predicted effects of N deposition in these 'up and coming' N-polluted regions. Some sources of uncertainty have been addressed in prior modeling analyses of N deposition, including the potential N taken up by plants following a decrease in N limitation of NPP (Townsend et al. 1996), the degree to which land-use and climate change modify a poten-tial N deposition response (Asner et al. 1997; Aber & Driscoll 1997), and the spatial and temporal patterns of N deposition itself (Holland et al. 1997). These aspects are still not well understood, but even less is known about geochemical, hydrological and multiple nutrient dynamics associated with N

transport following deposition. Few studies have focused on the fate of excess N deposition in systems outside of temperate forests, and, to our knowledge, no studies have tried to predict the most important factors controlling N transport and stabilization in humid tropical or semi-arid systems.

We present a new integrated terrestrial biophysics-biogeochemical process model, TerraFlux, and use this model to test the relative importance of factors that may strongly influence the NPP response of a hypothetical humid tropical evergreen forest and semi-arid savanna to anthropogenic N deposition. These factors include hydrological losses of dissolved inorganic and organic N, as well as multiple nutrient interactions with deposited inorganic N along the hydrological pathway. Few modeling efforts have addressed these factors, and no models have represented all of them in an integrated simulation frame-work. We carried out a series of sensitivity analyses using the TerraFlux model to aid in understanding the relative importance of these factors, and to highlight areas of particular sensitivity and uncertainty that could direct further experimental research.

Model analyses

The TerraFlux model simulates the fluxes and storage of C, water, and nutrients in vegetation and soils. The model has seven integrated modules including remote sensing, plant-soil radiative transfer, plant growth and carbon allocation, soil hydrology, soil solute transport, plant nutrient use, and soil carbon and nutrient cycling. Each of these modules is described in detail in Appendix 1. TerraFlux runs on a one-hour time step, and it simulates soil processes to a maximum depth of 10 m. Theoretically, the model can be set up for any number of nutrients if sufficient site-level data on plant requirement, plant-soil-microbial carbon:nutrient stoichiometry, and soil geochemical parameters are known. It thus can be employed with detail appropriate to landscape, regional and global analyses, as it is 1-dimensional and thus dependent only upon the spatial resolution of the input variables. However, we believe that too little information exists in the literature to allow for general analyses of multi-nutrient cycles in the plant-soil system. For this study, the model was run as a set of point simulations, without any spatially explicit representation of the input variables. We used the model to estimate the sensitivity of NPP to N deposition while 'turning on' the full N cycle for the semi-arid savanna simulations and both the N and Ca cycles for the humid tropical forest analyses. Variables used in these simulations are summarized in Appendix 2.

We developed two model sensitivity studies to assess the importance of physical, biological and geochemical controls over the potential NPP

response of humid tropical forests and semi-arid savannas to N deposition. These analyses were not intended to represent a particular geographic location, although most of the input parameters are based directly on published studies of these two ecosystem types. The primary goal of these sensitivity analyses was to evaluate the relative importance of a diverse set of factors involved in regulating an NPP response to simulated N deposition, and to develop a better sense for which factors deserve more attention in field studies related to N deposition. The factors considered are shown in Table 1, and these were varied individually across their plausible ranges based on available literature values.

A Monte Carlo analysis was used to quantify the absolute range of NPP responses resulting from variation in each factor (Table 1) at the end of a 50-year N deposition simulation (model spin-up with no N deposition plus 50 years of deposition). The Monte Carlo simulations were executed by randomly varying these factors (n = 500 runs per factor), then by ordering the factors by the sensitivity of the modeled ΔNPP (= [NPP_{end} − $NPP_{initial}$] / $NPP_{initial}$). A deposition rate of 5 kg NO_3^- ha^{-1} yr^{-1} plus 5 kg NH_4^+ ha^{-1} yr^{-1} was used in the semi-arid savanna simulations. This is based on the observation that semi-arid regions are experiencing increases in both nitrogen forms (Holland et al. 1993). A NO_3^- deposition rate of 10 kg NO_3^- ha^{-1} yr^{-1} was used for the humid tropical forest simulations based on atmospheric chemical transport predictions of future N deposition (Lelieveld & Dentener 2000). For the tropical forest simulations, special attention was given to both NO_3^- and Ca^{2+} because of the large amount of work that has been done on these interacting nutrients in temperate ecosystems (e.g., Likens et al. 1996; Stoddard et al. 1999). We focused the analysis on the uncertainty in the sorption kinetics of NO_3^- and Ca^{2+}, hydrological flow rates based on both precipitation variability and soil texture, and responses that could occur with changes in microbial uptake and soil carbon turnover.

In addition to the absolute uncertainty of each variable, we constructed a sensitivity analysis to quantify the relative contribution of each tested factor to an NPP response following chronic N deposition. Variables of interest (Table 1) were randomly selected within their respective range defined in the literature, and ΔNPP calculated following 50 years of NO_3^- deposition (called a base-case scenario). For every base-case ΔNPP scenario, each model variable in Table 1 was, in turn, perturbed by ± 10% of its measured range, and the simulation repeated. The ± 10% range was selected based on the notion that a smaller change in each variable would be difficult to detect using most field methods. A database was created for all model simulations (n = 500 base-case ΔNPP + 500 × 14 perturbed parameters of ΔNPP = 7,500 TerraFlux ΔNPP simulations). The sum of the squares of differences,

Table 1. Biological, geochemical and hydrological parameters selected to vary in the Terra-Flux sensitivity analyses to N deposition. Value ranges are taken from the literature sources indicated

Parameter	Lowland Humid Tropical Forest	Semi-arid Grassland	Example Literature Source
Climate			
Surface Temperature	+/– 10% of Figure 1a	+/– 10% of Figure 1d	ECMWF (1998)
Precipitation	+/– 20% of Figure 1b	+/– 20% of Figure 1e	ECMWF (1998)
Inputs			
NO_3 Deposition	0–10 kg $ha^{-1}yr^{-1}$	0–10 kg $ha^{-1}yr^{-1}$	Holland et al. (1999)
NH_4 Deposition	—	0–10 kg $ha^{-1}yr^{-1}$	Holland et al. (1999)
Vegetation			
Foliar C:N	20–40	40–60	Parton et al. (1994)
Fine Root C:N	20–40	40–60	Gordon and Jackson (2000)
Foliar N Resorption Eff.	70–90%	85–95%	Vitousek (1982, 1984), Killingbeck (1996),
Foliar Ca Resorption Eff.	70–90%	N/v	Aerts (1996)
Nitrogen Fixation Rate	1.5–3.5 g m^{-1} yr^{-1}	0.2–0.8 g m^{-1} yr^{-1}	Cleveland et al. (1999)
Soils			
Texture	Clayey to Sandy*	Clayey to Sandy**	
Microbial C:N	8–12	8–12	Paul and Clark (1996)
Microbial C:Ca	30–50	N/v	Inferred from Staff and Berg (1982)
Slow SOC C:N	10–20	10–20	Parton et al. (1994)
Slow SOC C:Ca	80–100	N/v	Cromack (1973), Staaf and Berg (1982)***
NO_3 Isotherms: 'A' parameter	$8e10^{-5}$–$2e10^{-3}$	$8e10^{-5}$–$2e10^{-3}$	Cahn et al. (1992)
Ca Isotherms: 'A' parameter	$1e10^{-3}$–$3e10^{-3}$	N/v	Marcano-Martinez and McBride (1989)
NH_4:NO_3 Partitioning	1:5 to 1:10	1:1 to 1:5	Vitousek and Matson (1988), Blair (1997)

N/v = parameter not varied in scenario
* = Texture in tropical forest scenario was varied from 80% clay/10% sand to 10% clay/80% sand
** = Texture in grassland scenario was varied from 70% clay/15% sand to 20% clay/50% sand
*** = No available data on fractionated SOC C:Ca, thus we assumed that values were roughly similar to that of litter C:Ca

or merit-of-change value, between the original 50-year ΔNPP and the 50-year ΔNPP derived following each parameter perturbation was recorded. A principal components analysis (PCA) was then performed on the merit-of-change values. Since the first principal component axis represents the direction of maximum variance, the weighting of each perturbed parameter's contribution to that axis was a measure of the model's sensitivity to the perturbed variable (Asner 1998). Thus, a sensitivity index was derived for all variables. This entire procedure was repeated at N deposition rates ranging from 0–20 kg ha^{-1} yr^{-1}, providing a comparison of ecosystem responses to increasing N deposition over time.

Results and discussion

Vegetation and soil parameters used in these analyses are provided in Table 1 and Appendix 2. Appendix 2 shows the full listing of TerraFlux model input parameters and their typical values for semi-arid savanna and humid tropical forest environments. Table 1 shows the subset of parameters and their specific range used in the sensitivity analyses. These values were selected from representative literature sources (given in Table 1) to estimate their ecologically and biogeochemically plausible range. This step is important because any modeling analysis of the relative importance of parameters depends strongly upon the value ranges of the input parameters.

For the base-case scenarios, we used the hourly temperature, precipitation and downwelling shortwave radiation shown in Figure 1. These values were taken from the ECMWF Climate Reanalysis Program (ECMWF 1998); the humid tropical system (Figure 1(a–c)) has the typical aseasonal temperature regime, a 2470 mm per year rainfall cycle, and a relatively constant shortwave radiation regime. Rainfall and radiation are almost inversely correlated. The semi-arid savanna climate (Figure 1(d–f)) shows a typical northern hemisphere seasonal temperature and radiation cycles, and an episodic rainfall regime.

The resulting hourly ΔNPP, soil respiration, and 0–30 cm water flux are shown in Figure 2. ΔNPP of the tropical forest was 1163 g m^{-2} yr^{-1} (Figure 2(a)), which is very typical of these ecosystems (Scurlock et al. 1999); ΔNPP was almost balanced by an annual heterotrophic respiration (R_h) rate of 1155 g m^{-2} yr^{-1} (Figure 2(b)). The net ecosystem production (NEP) of this system was therefore about 8 g m^{-2} yr^{-1}, or slightly aggrading. The savanna ΔNPP varied strongly by both season and precipitation events (Figure 2(d)), and the annually integrated ΔNPP value was 460 g m^{-2} yr^{-1}. This was balanced by a soil CO2 respiration rate of 460 g m^{-2} yr^{-1} (NEP $\approx$ 0). Soil water fluxes were often very high in the tropical forest setting (Figure 2(c)), reaching saturated
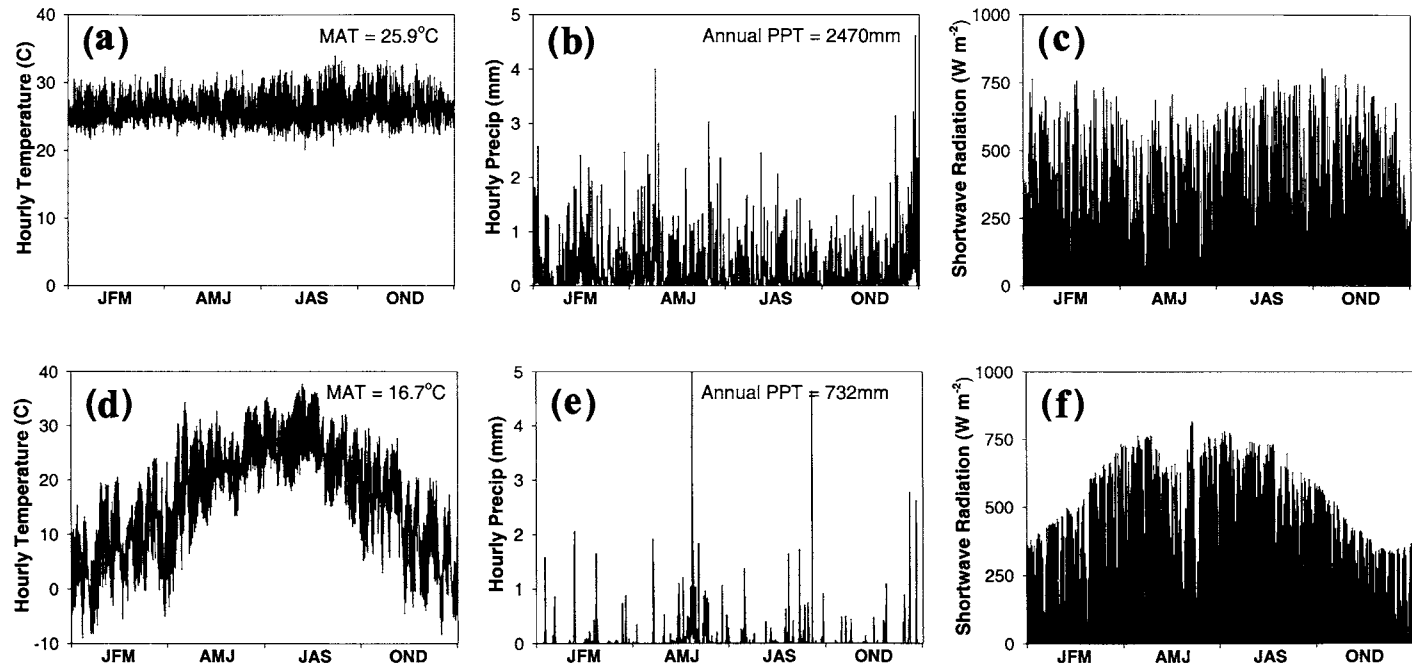
Figure 1. Hourly input climate data for TerraFlux simulations of a lowland humid tropical forest and a semi-arid savanna/grassland. These datasets are taken from the ECMWF Climate Reanalysis (ECMWF 1998). (a)–(c) Temperature, rainfall, and downwelling solar radiation from 1990 at 3°S, 60°W (West-Central Amazon Basin). (d)–(f) Temperature, rainfall, and downwelling solar radiation from 1990 at 34°N, 99°W (North Texas mesquite savanna). MAT = mean annual temperature.
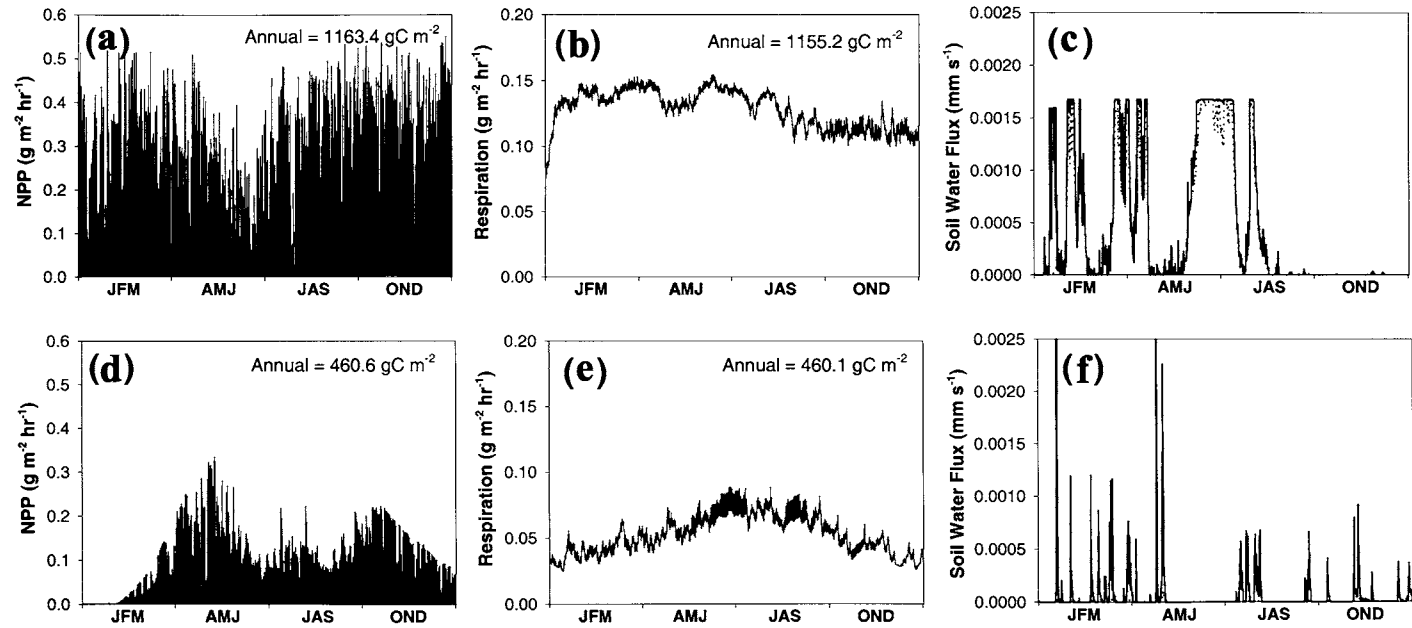
Figure 2. Hourly NPP, heterotrophic respiration, and soil water flux at 0–10/10–30cm depths at the end of the model spin up, prior to the onset of 50 years of NO_3^- deposition. (a)–(c) Lowland humid tropical forest. (d)–(f) Semi-arid savanna/grassland.

hydraulic conductivity in the top soil layers while the excess water inputs were removed as runoff (not shown). Savanna soil water fluxes varied sharply with rainfall events (Figure 2(f)).

For the subsequent tropical forest simulations, we found it necessary to parameterize the fraction of leachable NO_3^- that could bond to Ca^{2+}. Independent of the soil sorption affinity for NO_3^- or Ca^{2+}, the fraction of NO_3^- or Ca^{2+} that actually makes contact in solution within a soil layer is difficult to measure in actual ecosystems. If the entire amount of NO_3^- in solution bonds with all free Ca^{2+} at any given time, then the strongest calcium loss pathway develops. Alternatively, if only a fraction of the NO_3^- makes contact with Ca^{2+}, then the potential for loss is reduced.

Figure 3 shows the sensitivity of the simulated tropical forest NPP and soil organic carbon (SOC) content to assumed levels of interaction between leached NO_3^- and soil solution/sorbed Ca^{2+}. Assuming that 25% of the solution NO_3^- interacts with solution Ca^{2+} within each soil layer results in a 12% and 6% decrease in NPP and SOC, respectively, after 50 years of 10 kg ha^{-1} yr^{-1} NO_3^- deposition. Increasing the interaction term to 50% leads to NPP losses of 21% and SOC decreases of 11% from pre-deposition values. These results emphasize both the striking effect of NO_3^- leaching in the model and the importance of the uncertainty in simulating soil solution anion-cation interactions in a general biogeochemical model. Therefore, we flagged this parameter as vitally important in future studies of N deposition effects on terrestrial ecosystems, especially those found in the humid tropics. For subsequent analyses, we fixed this parameter to a value of 25%.

Absolute sensitivity

The absolute sensitivity of the model to climate, hydrological, biological and geochemical parameters is shown in Figure 4, and is based on the value ranges presented in Table 1. For each tropical forest simulation, NO_3^- was deposited for 50 years at a rate of 10 kg ha^{-1} yr^{-1}. The semi-arid savanna simulations had 5 kg ha^{-1} yr^{-1} of NH_4^+ and 5 kg ha^{-1} yr^{-1} of NO_3^- for 50 years. The % ΔNPP values shown in Figure 4 were always negative in the tropical forest simulations and positive in the semi-arid savanna simulations. Of all parameters tested in the tropical forest analysis, the dominant drivers of NPP response to N deposition were, in descending order of importance: soil hydrological flow, foliar Ca resorption efficiency, nitrification rate (represented by the fraction of mineralized N that becomes NO_3^-), soil affinity for Ca sorption, soil affinity for NO_3^- sorption, and biological N fixation rate. For the semi-arid savanna simulations, NPP response to N deposition was most dependent upon: precipitation, soil hydrological flow, biological N fixation rate, foliar N resorption efficiency, and temperature.
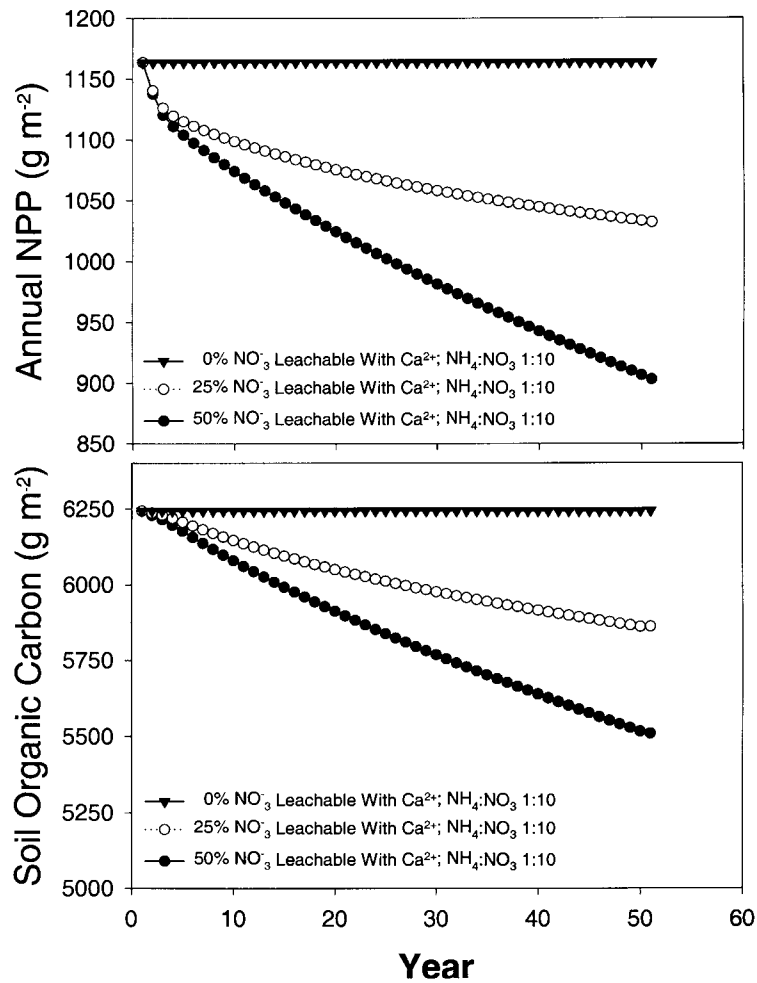
12

Figure 3. Modeled NPP and soil carbon storage response to 50 years of NO_3^- deposition in the tropical forest simulation assuming three levels of NO_3^-/Ca^{2+} interaction in soil solution. For all subsequent simulations, a conservative guess of 25% interaction was employed.

Only the six most important factors for each simulated ecosystem will be discussed. However, we note that the top eight factors in the tropical forest analyses are not represented in most terrestrial biogeochemical models (e.g., Parton et al. 1987; Running et al. 1994; Potter et al. 1993) and none are represented in N deposition response models (e.g., Townsend et al. 1996; Holland et al. 1997). Also, as noted above, we feel there is too little information to reasonably simulate a full suite of biologically important nutrients and their interactions with excess N; our analysis of N and Ca here is merely
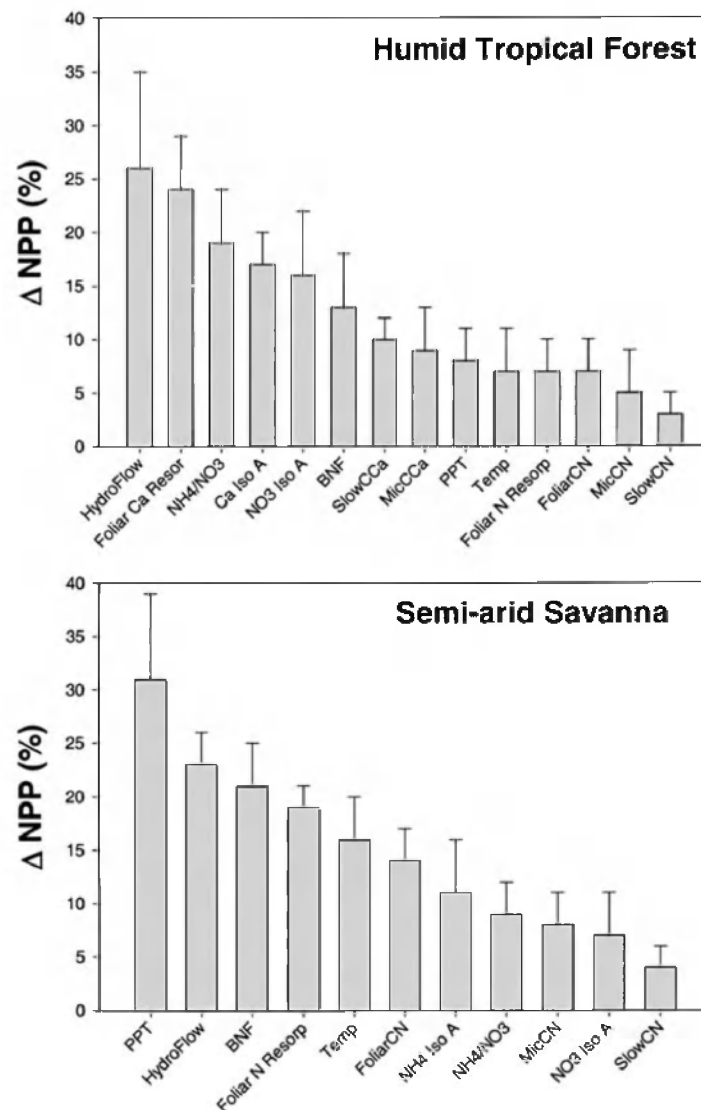
Figure 4. Absolute sensitivity of TerraFlux in humid tropical forest (top) and semi-arid savanna scenarios using ranges of parameters listed in Table 1. Key: HydroFlow = soil water flux in top 0–30 cm; Foliar Ca Resor = foliar Ca resorption efficiency; NH_4:NO_3 = partitioning of mineralized nitrogen to ammonium and nitrate; Ca Iso A: soil sorption affinity for Ca^{2+} (Appendix 1); NO_3 Iso A = soil sorption affinity for nitrate; BNF = biological nitrogen fixation; SlowCCa = C:Ca ratio of slow organic matter pool; MicCCa = C:Ca ratio of microbial biomass; PPT = precipitation; Temp = temperature; Foliar N Resorp = foliar N resorption efficiency; Foliar CN = foliar C:N ratio; MicCN = C:N ratio of microbial biomass; SlowCN = C:N ratio of slow organic matter pool; NH_4 Iso A: soil affinity for NH_4^+.

meant to be illustrative rather than prognostic. In reality, interactions with multiple elements, including pH changes and their affects on nutrients such as P (Matson et al. 1999), are all likely to contribute to the response of ecosystems to excess N, especially in humid tropical systems. Again, virtually none of these interactions are represented in widely used ecosystem models.

In TerraFlux, soil hydrological flow (HydroFlow in Figure 4) is modeled on an hourly timestep and is a function of soil texture, hydraulic conductivity and soil matric potential (Appendix 1). HydroFlow was the most important parameter in determining the N deposition/NPP response of the tropical forest site to N deposition, and it was the second most important parameter for the savanna site (second to precipitation). In the tropical forest simulations, hydrological flow played a central role in mediating the transport of NO_3^-, which had a major impact on calcium losses. In the savanna simulations, hydrological flow and precipitation played dominant roles in regulating the degree to which moisture constrains NPP, and in the amount of N maintained in the system for subsequent use by plants (instead of being lost in episodic leaching events). Thus, hydrological flow played vital but very different roles in regulating an NPP response to N deposition in these contrasting ecosystems.

Foliar Ca^{2+} resorption efficiency also played a major role in regulating the effects of N deposition on tropical forest NPP. Resorption was varied within the ranges reported by Vitousek (1984), and high resorption efficiency reduced the amount of mobile Ca in the soils, and therefore reduced NO_3^--driven Ca^{2+} losses. The fraction of mineralized N that became NO_3^- (versus NH_4^+) was also important in determining the NPP response. However, studies show that most mineralized N is nitrified in relatively N-rich humid tropical ecosystems (e.g., Vitousek & Matson 1988), therefore our specified range of NH_4^+: NO_3^- between 1:5 and 1:10 may be liberal. Had this ratio been constrained to a narrower range of variability, its importance would have diminished significantly (results not shown).

The "A" terms in the calcium and nitrate isotherms, which represent the overall sorption affinity of the soil for these nutrients (Appendix 1), were the next most important parameters in the tropical forest analysis. Increased sorption affinity resulted in increased stabilization of Ca^{2+} and NO_3^- on soil exchange sites, which dampened the NO_3^--Ca^{2+} loss effect on NPP. However, these parameters have an explicit time-dependence, making it difficult to estimate how important they would be at other N deposition rates and/or longer timescales of deposition (see next section).

Finally, the amount of nitrogen coming into the plants via biological fixation (BNF) had an unexpectedly large effect on the NPP response of the tropical system to N deposition. This result is interpreted as a pre-

existing (model-equilibrated) dependence of plant productivity on BNF in these systems. A change in this dependence following N deposition (e.g., decreased dependence on BNF) results in increased NO_3^- uptake and thus less NO_3^- leaching and Ca^{2+} loss. We note that interactions between increasing N deposition and BNF are quite possible (Vitousek & Field 1999), but information on such responses is sparse in the literature, and TerraFlux does not adjust BNF in response to changing N availability.

As discussed, the principal drivers of NPP response to N deposition in the semi-arid savanna simulations were precipitation and soil hydrological flow. These parameters appear to be dominating factors somewhat independent of the 10 kg ha^{-1} yr^{-1} $NH_4^+ + NO_3^-$ deposition rate. In this case, both water and N availability appear to be co-limiting to plant productivity. An increase in moisture availability to plants via increased rainfall and/or decreased hydrological losses results in an increased capability for plant uptake of deposited N. However, at very high precipitation or soil water flow rates, incoming N becomes less available for plant uptake and the NPP response is weakened. Thus, there is an important hydrological-biogeochemical feedback regulating the potential fertilizing effect of N in these semi-arid savanna simulations.

BNF played a major role in determining NPP variability in the semi-arid system as well, again somewhat independent of the N deposition simulation itself. Cleveland et al. (1999) have summarized the strong dependence of arid and semi-arid ecosystems on biological N fixation, showing that N fixation (via either symbiotic or free-living organisms) could potentially contribute more than 70% of the N required to support NPP in these systems. Again, as we do not a have feedback mechanism in the model to inhibit biological nitrogen fixation if N becomes less limiting (via deposition), we cannot assess the importance of indirect changes in N uptake resulting from N enrichment. However, we can speculate that atmospheric inputs of N could decrease plant reliance on N-fixers.

Foliar N resorption efficiency played a predictable and important role in determining the NPP variability of the savanna simulations. This concurs with the report by Killingbeck (1996) that demonstrates high N resorption in plants from these environments. Finally, temperature was the fifth most important factor determining the NPP variability in these simulations; this effect has been incorporated into previous N deposition modeling studies (e.g., Townsend et al. 1996; Holland et al. 1997).

Relative sensitivity

The absolute sensitivity of the model to variation in input parameter values indicates which factors may be important to consider in future N deposition studies. However, such an analysis does not provide a means to under-
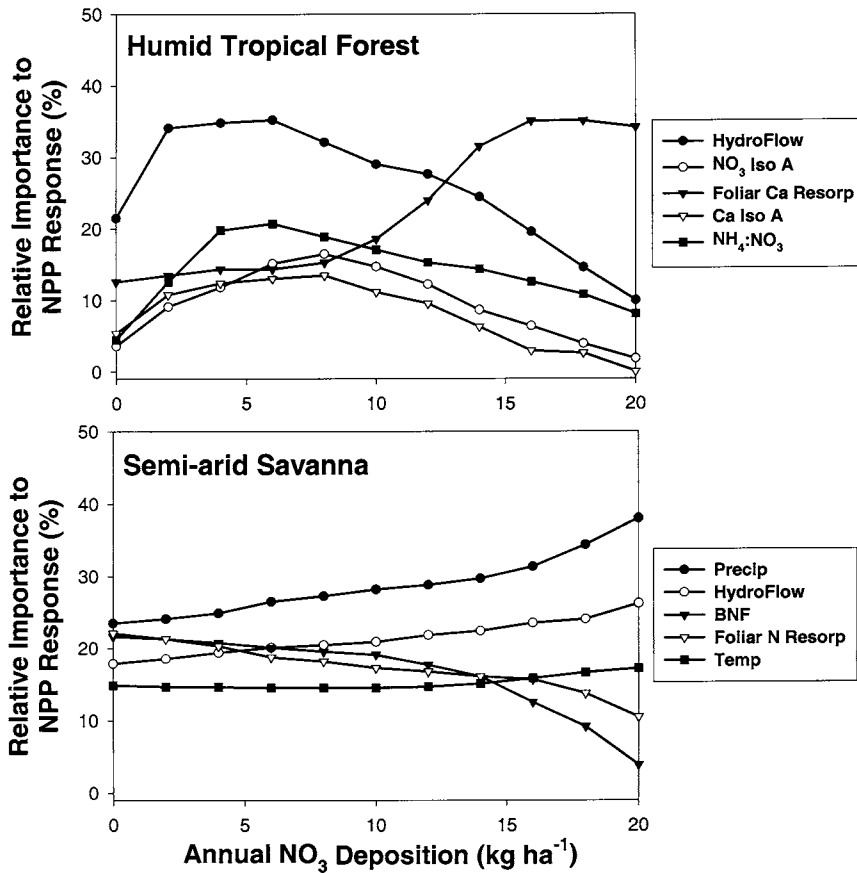
Figure 5. Relative importance of top five factors from Figure 4 in determining a NPP response to varying levels (0–20 kg ha^{-1} yr^{-1}) of chronic nitrogen deposition (50 year simulations). See Figure 4 for parameter definitions.

stand the relative importance of these factors through time. The sensitivity analysis presented here highlights how the uncertainty in model parameters can change with increasing N deposition rate. In these analyses, NO_3^- was deposited at increasing rates from 0–20 kg ha^{-1} yr^{-1} for 50 years, and the relative sensitivity was calculated as explained in the Methods section. Only the five most important parameters from Figure 4 are presented.

Three interesting trends emerged in the tropical forest analysis associated with hydrological, biological, and geochemical processes in the model (Figure 5). First, the relative importance of hydrological flow changed dramatically with increasing N deposition. Hydrological transport of NO_3^- was the primary factor controlling the NPP response to N enrichment when

deposition levels were between 0-6 kg ha^{-1} yr^{-1}. It then steadily decreased in importance as N deposition rates became very high (6–20 kg ha^{-1} yr^{-1}). The point at which hydrological flow decreases in relative importance represents a threshold at which water flow through the soil no longer dominates the NO_3^--Ca^{2+} loss process. At this theoretical point, nitrate levels are sufficiently high to drive a negative ΔNPP response that decreases in dependence upon the flow rate.

An opposing trend emerged in the role of foliar Ca^{2+} resorption efficiency in the tropical forest simulations (Figure 5). At lower NO_3^- deposition rates (< 6 kg ha^{-1} yr^{-1}), variability in calcium resorption resulted in about a 12% variation in NPP response. The relative importance of Ca^{2+} resorption increased non-linearly as NO_3^- deposition and NO_3^--Ca^{2+} losses increased, peaking at a deposition rate of about 16 kg ha^{-1} yr^{-1}. At this point, even a small change in Ca^{2+} resorption efficiency has a very large effect on NPP response to N deposition because, at that point, soil pools of available Ca^{2+} are extremely low. At NO_3^- deposition rates greater than 16 kg ha^{-1} yr^{-1}, the relative importance of Ca^{2+} resorption efficiency leveled off, indicating the maximum extent of the plant's biological ability to cope with Ca^{2+} losses resulting from NO_3^- deposition.

The relative importance of NO_3^- and Ca^{2+} sorption in soils peaked at NO_3^- deposition values of about 6–8 kg ha^{-1} yr^{-1} then slowly declined with increasing deposition rates. This result highlights the relatively low NO_3^- and Ca^{2+} sorption capacity of highly weathered soils (as depicted in the range of NO_3^- and Ca^{2+} sorption isotherm parameters from the literature: Table 1). Although these soils often have a relatively high anion exchange capacity (e.g., especially for PO_4^-), the NO_3^- sorption isotherms available for use from the literature (e.g., Cahn et al. 1992) do not indicate sufficient stabilization capacity for soils to significantly buffer against NO_3^- increases resulting from deposition. However, we recognize that there are still too few studies to conclude that NO_3^- sorption plays the relatively constrained role as depicted in the tropical forest simulations shown in Figure 5.

The degree to which nitrification occurs (represented here as a NH_4^+:NO_3^- ratio) in tropical systems played a role similar to those of the affinity parameters in the sorption isotherms. In these analyses, we varied NH_4^+:NO_3^- from 1:5 to 1:10; This parameter's contribution to an NPP response peaked at NO_3^- deposition rates of 5–6 kg ha^{-1} yr^{-1} (Figure 5). It then declined with higher deposition rates, in part because we simulated all excess N inputs to the tropical system as nitrate. Had we assumed that a very high fraction of total mineralized N undergoes nitrification (Vitousek & Matson 1988), then its relative importance in controlling an NPP response to any NO_3^- deposition rate would have remained low throughout the model experi-

ment. In contrast, if a significant portion of mineralized N in such systems is cycled as NH_4^+ and is not nitrified, the effects on cation loss would decline. Such uncertainty becomes even more critical if future increases in N loading to tropical systems do involve significant levels of reduced N deposition. Thus, we again emphasize the importance of knowing the ecologically and biogeochemically plausible range of values used to develop a sensitivity analysis. We also highlight the importance of further experimental research to decrease the uncertainty in simulating these processes. This is particularly pertinent for nitrification, because at this time a general model for nitrifier efficiency has not been developed. Nitrification rates are therefore relegated to a parameterization in a general model such as we have done here.

The semi-arid savanna simulations show dramatically different trends than those described for the tropical forest analyses. There were two dominant trends in the five parameters (top 5 from Figure 4) tested in this analysis. First, the relative importance of precipitation inputs and hydrological flow actually increased as NO_3^- deposition increased (Figure 5). A check of the soil organic and inorganic N pools indicated that this trend was due to a reduction in the strength of nitrogen limitation of NPP at high deposition rates. The change observed in Figure 5 is mild but ecologically significant; it implies that at high N deposition rates, the more arid systems will switch from water-nitrogen co-limitation to a system increasingly constrained only by water availability.

The second dominant trend in the semi-arid analysis was a decrease in the role of the biota in regulating N cycling, especially the pre-existing mechanisms that cope with a nitrogen scarce environment. The relative importance of foliar N resorption efficiency and biological N fixation decreased non-linearly with increasing NO_3^- deposition (Figure 5). As deposition rates increased from 0–10 kg ha^{-1} yr^{-1}, foliar N resorption and BNF only slowly decreased their role in determining a NPP response. Once the deposition rates exceeded 10 kg ha^{-1} yr^{-1}, the relative importance of these two parameters sharply decreased, again indicating that the system switched from an N-limited system strongly dependent on N retention and biological input pathways to one more limited by water availability alone.

Conclusions

Nitrogen deposition is increasing worldwide, and both humid tropical and semi-arid ecosystems are increasingly being exposed to new inputs of anthropogenically-derived nitrogen (Holland et al. 1999; Matson et al. 1999). Emerging problems of N pollution in these environments call for experimental analyses to quantify the relative importance of the mechanisms controlling ecosystem responses to N enrichment. Comparative work on the

similarities and differences between semi-arid, tropical and the better-studied temperate forest ecosystems is also critically needed. At the same time, the models that are used to spatially and temporally extend experimental findings to broader scales must be improved to better represent the hydrological, biological, and geochemical controls over the system responses to N perturbations.

The TerraFlux model represents a step from the more typical box representations of water and nutrient dynamics that are prevalent in biogeochemical modeling to a framework that places paramount emphasis on transport and the biological-geochemical competition for nutrients. TerraFlux is only a first step, and many improvements are needed to make the model simulate nutrient transport in a more realistic way. Many of the current problems with the model result from a lack of experimental information on multi-nutrient sorption interactions and competition with soil exchange sites, preferential or by-pass flow pathways for episodic water transport, and microbial functionality and the role of mychorrhizae in regulating nutrient cycles. These model deficiencies point to areas of general biogeochemical research requiring much more attention in field and laboratory analyses.

In the more specific case of N deposition, the analyses presented in this paper highlight the factors critical to determining plant response to N enrichment. Within the scope of the processes represented in the model, the following variables emerged as most important and least understood from an experimental point of view:

- Fraction of soil solution NO_3^- that bonds with soil solution cations such as Ca^{2+}.
- Hydrological flow patterns of deposited N through soils.
- Soil geochemical control over N and other nutrient losses: e.g., soil sorption and stabilization capacity.
- Soil biological mechanisms of nutrient uptake and retention.
- The relative importance of nitrification across ecosystems, and changes in nitrification rates with NH_x and NO_y deposition.

Until we are able to better quantify these variables, our ability to incorporate them into a physically and biogeochemically consistent modeling framework will be severely limited. As well, we note that the above list of uncertainties is derived from the already restricted set of conditions we felt able to simulate; Information on excess N interactions with other elements and soil pH is conspicuously lacking. Moreover, it is also important to note that these simulations did not address the interesting observation that nitrogen often appears to leach in organic forms from temperate forest ecosystems (e.g., Seely & Lajtha 1997), indicating that the soil microbial community processes deposited inorganic N prior to loss from the system. Similarly, a

20

dominant form of nitrogen mobility in arid ecosystems appears to be as DON (e.g., Schlesinger et al. 1999, 2000). Therefore, the partitioning of leached nitrogen into organic and inorganic forms will be require an integration of field data with additional model simulations. As is, the simulations presented here probably push the limit of our current knowledge base for developing prognostic analyses of how N deposition will impact semi-arid and humid tropical ecosystems. Nonetheless, we believe that these analyses are a useful first step for bringing the most pressing and difficult issues to the forefront, and for developing a set of additional goals for the biogeochemical research community.
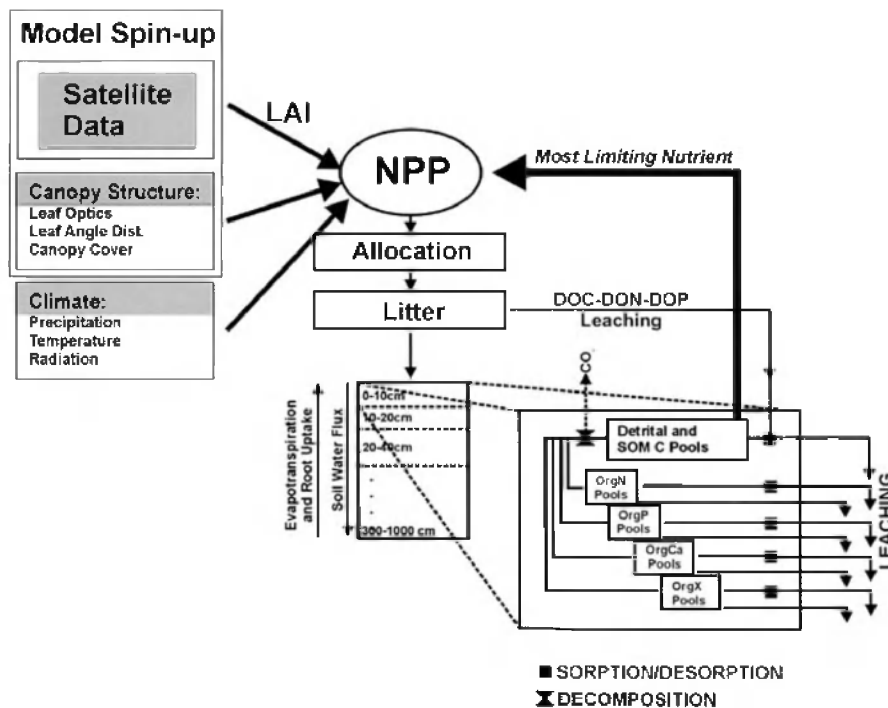
Acknowledgements

Appendix 1: The TerraFlux Model

Remote sensing and radiative transfer

In TerraFlux, plant canopy leaf area index (LAI) is critical to deriving canopy photosynthetically active radiation absorption (fPAR), net primary production (NPP), evapotranspiration, canopy thermal load, soil hydrology, plant phenology (e.g., litterfall), canopy nutrient uptake and resorption, and throughfall concentrations of dissolved C and nutrients (Figure A1). Therefore, the model places emphasis on the accurate (or realistic) estimation of LAI in time-series. LAI is estimated on a multi-temporal basis from satellite data using a radiative transfer (RT) inverse modeling algorithm (Asner et al. 1998a); the NOAA Advanced Very High Resolution Radiometer (AVHRR) is employed in global applications of this approach. In the forward mode, the RT sub-model is described by:

$$\rho_{canopy} = f(\text{LAI}, \text{LAD}, \rho_{leaf}, \rho_{leaf}, \rho_{soil/litter}, \theta_{Sun}, \phi_{Sun}, \theta_{view}, \phi_{view}) \tag{1}$$

where ρ_{canopy} is a satellite estimate of surface reflectance, LAD is the leaf angle distribution, ρ_{leaf} and τ_{leaf} are leaf reflectance and transmittance, respectively, $\rho_{soil/litter}$ is the reflectance of either exposed soil or surface litter, and $\theta_{Sun}, \phi_{Sun}, \theta_{view}, \phi_{view}$ represent the Sun and viewing geometry. The model is run in an inverse mode as LAI is iteratively adjusted until a best match between the simulated and actual satellite signatures is achieved (Figure A2). During the RT model inversion process, leaf angle distribution is fixed by vegetation type (Appendix 2), and Sun-view geometry is known from the satellite ephemeris data. Leaf optical properties and soil/litter surface reflectance are constrained during the inversion using the
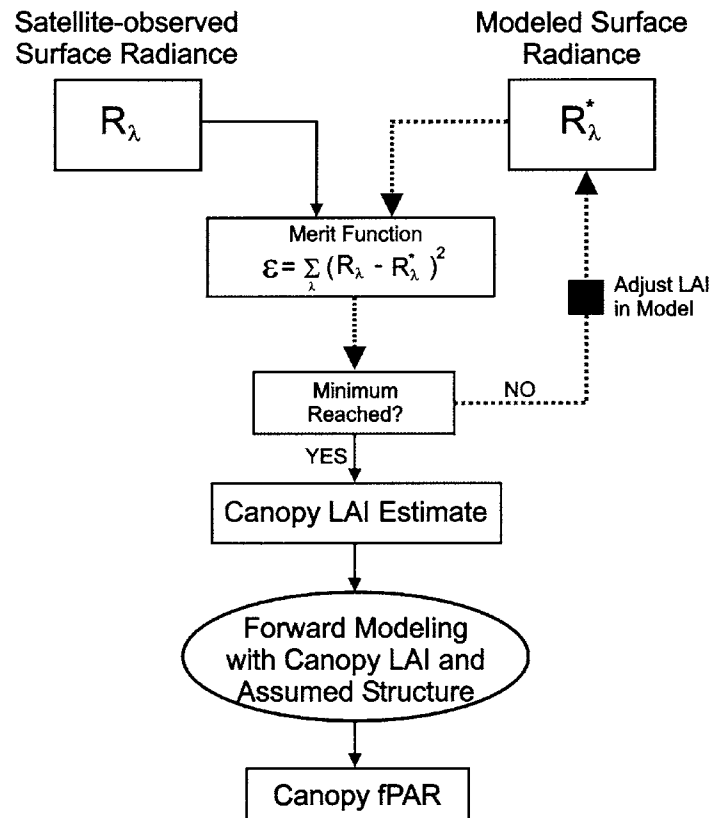
Model Spin-up

Satellite Data

LAI

NPP

Most Limiting Nutrient

Canopy Structure:
Leaf Optics
Leaf Angle Dist.
Canopy Cover

Allocation

Climate:
Precipitation
Temperature
Radiation

Litter

DOC-DON-DOP
Leaching

Evapotranspiration and Root Uptake

Soil Water Flux

0-10cm
10-20cm
20-40cm
300-1000 cm

Detrital and SOM C Pools

OrgN Pools

OrgP Pools

OrgCa Pools

OrgX Pools

LEACHING

■ SORPTION/DESORPTION
✕ DECOMPOSITION

A1. General schematic of the TerraFlux biophysics-biogeochemical process model. Although any nutrient important to plant growth can be simulated, only nitrogen and calcium (humid tropical forest simulations) were employed here. Satellite-derived estimates of leaf area index (LAI) area used to estimate NPP in the initial 'spin-up' phase of a simulation, followed by transition to the NPP calculations driven by climate, nutrient availability, and vegetation structure.

databases developed by Asner (1998) and Asner et al. (1998b). The specific RT sub-model equations and inverse solution are discussed by Asner et al. (1998a).

A particularly useful aspect of TerraFlux is that assumptions about canopy architecture (e.g., leaf angle distribution) and leaf optical properties used within this RT inversion sub-model also affect calculations of evapotranspiration, canopy energy balance, and carbon cycling in other sub-models (described below). That is, this remote sensing approach is integrated with the equations determining material and energy transport used in other parts of the overall model, allowing for implicit checking of the physical and biogeochemical plausibility of parameters across many simulated processes in the model.

Canopy-soil energy balance

Following the LAI estimate, the radiative transfer model is run in forward mode to estimate $fPAR_{foliage}$ every hour based on the principle of photon scattering in canopies. The equations for this process are provided in detail by Asner and Wessman (1997), but are based on the observation that $fPAR_{foliage}$ is a function of not only LAI but also solar angle, leaf optical properties, canopy architecture (e.g., leaf angle distribution), and soil/surface litter reflectance

A2 . During model spin-up, time-series (e.g., every 10 days) satellite estimates of leaf area index (LAI) play a major role in constraining calculations of canopy photosynthetically active radiation absorption (fPAR), net primary production (NPP), evapotranspiration, canopy thermal load, soil hydrology, plant phenology (e.g., litterfall), canopy nutrient uptake and resorption, and hroughfall concentrations of dissolved C and nutrients. A method is used to estimate LAI by inverting a mechanistic canopy radiative transfer model. The model simulates satellite observations of vegetation and soils using input parameters of LAI, canopy structure, leaf optical properties, soil/surface litter reflectance and solar/viewing geometry. The model is run iteratively (dotted lines) to find the LAI estimate that results in the best model fit to the satellite observations.

(Asner et al. 1998a). Three dimensional radiation transport in the canopy is simulated to allow for the anisotropic absorption of photons by foliage, wood, litter and soil surfaces.

Canopy and soil net radiation is calculated using the algorithms described by Bonan (1996). These are based on factors including canopy aerodynamic resistance (Bonan 1994), shortwave and longwave radiative transfer, and Monin-Obukhov similarity theory (Brutsaert 1982; Arya 1988). Canopy and soil temperatures are important for calculating evapotranspiration rates, and these too are modeled using equations detailed by Bonan (1996).

Plant growth, allocation & litterfall

Net primary production (NPP) is calculated using a variant of the method detailed by Field et al. (1995):

$$NPP = fPAR_{foliage} \bullet PAR_I \bullet \varepsilon^* \bullet W_s \bullet T_s \bullet N_s \tag{2}$$

where $fPAR_{foliage}$ is the fraction of photosynthetically active radiation (PAR) absorbed by green foliar component of the canopy and PAR_I is the total downwelling PAR. The calculated light use efficiency (ε) is derived at each timestep by down-regulating the global light use efficiency (ε^*) of Field et al. (1995) by W_s, T_s, and N_s: the effects of water, temperature and nitrogen stress on plant growth, respectively. The factors W_s and T_s range from 0.5–1.0 and from 0.8–1.0, respectively, and are calculated in a similar way to Potter et al. (1993), but the physical modeling of soil moisture is more mechanistically based on Richards' hydrological flow described below. The nitrogen stress factor (N_s) is scaled from 0.8–1.0 based on the difference between the nitrogen demand to support NPP and the inorganic nitrogen availability in the soil, also described below. The satellite-driven NPP algorithm is only used during model 'spin-up' to set the initial model conditions; it is turned off following the spin-up process to allow a dynamic simulation of the NPP response to water, energy and nutrient perturbations, as described below.

NPP is allocated to foliage, wood, and roots based on Friedlingstein et al. (1999) with some modification to allow for both coarse and fine root growth. Once allocated to the belowground plant pool, this carbon is distributed throughout the root system according to the biome-dependent distributions of Jackson et al. (1997) or by site-level knowledge. The fraction of the total root growth per layer and per time step is then divided into fine and coarse fractions based on an input parameter to the model. For general modeling purposes, this value is set to 90% for fine roots. The timing and amount of foliage litterfall is estimated using the algorithm described in detail by Randerson et al. (1997). This algorithm utilizes the temporal shape of the time-series LAI derived from the satellite data. Root turnover is simulated in parallel to foliage turnover, and wood losses are based more simply on an annual turnover rate (Parton et al. 1987).

Plant nutrient use

Foliar N and P resorption proficiency (e.g., g N/g litterfall) is based on the global syntheses of Killingbeck (1996) and Aerts (1996). Foliar Ca, Mg and K resorption proficiency is based on a similar study by Asner and Matson (*in prep.*). Root and wood nutrient resorption are held constant to 5% of the total nutrient flux in root and wood turnover (e.g., root loss * $N:C_{roots}$) since these losses are usually episodic and therefore inefficiently managed by plants (Gordon & Jackson 2000). The nutrient:C ratio of plant parts are fixed; nitrogen:C is provided by Parton et al. (1994) and Killingbeck (1996), and all other nutrient:C ratios were developed by Gordon and Jackson (2000) and Asner and Matson (*in prep.*). Plant nutrient requirement therefore represents the nutrient needed to meet NPP demand and to maintain the nutrient:C ratio of leaves, wood and roots, after accounting for nutrient resorption by foliage, wood and roots:

$$
\begin{aligned}
\text{Nutrient requirement} \;=\; &[(NPP_{foliage} \bullet \text{nutrient}:C_{foliage})+ \\
&(NPP_{wood} \bullet \text{nutrient}:C_{wood})+ \\
&(NPP_{roots} \bullet \text{nutrient}:C_{roots})]-
\end{aligned}
\tag{3}
$$

$$[\text{Nut resorp}_{\text{foliage}} + \text{Nut resorp}_{\text{wood}} +$$
$$\text{Nut resorp}_{\text{root}}]$$

Soil hydrology

Soil moisture and water flow are simulated using the formulation of Bonan (1996). We briefly describe only the key components of this approach that affect the results reported in this paper. Incoming water (e.g., precipitation) can evaporate from the canopy surface, infiltrate into the soil column or be lost as surface runoff. The amount of throughfall is a function of leaf area index (from the satellite data) and evaporative losses from the canopy (from the energy balance equations of Bonan 1996). The partitioning of the total water input at the soil surface (from throughfall and snowmelt) to infiltration and surface runoff is based on the water content of the top soil layer and its saturation point (w = $\theta/\theta_{\text{sat}}$), where θ is volumetric water content (mm^3 H$_2$O/mm^3 soil layer). Soil water in each layer is calculated from the conservation equation:

$$\frac{\Delta\theta\Delta z}{\Delta t} = -q_i + q_o - e \tag{4}$$

where Δz is the layer thickness, Δt is the model time step (1 hour), e is the evapotranspiration loss from the layer (mm s^{-1}), q_i is the water flux into the layer, and q_o is the water flux out of the layer.

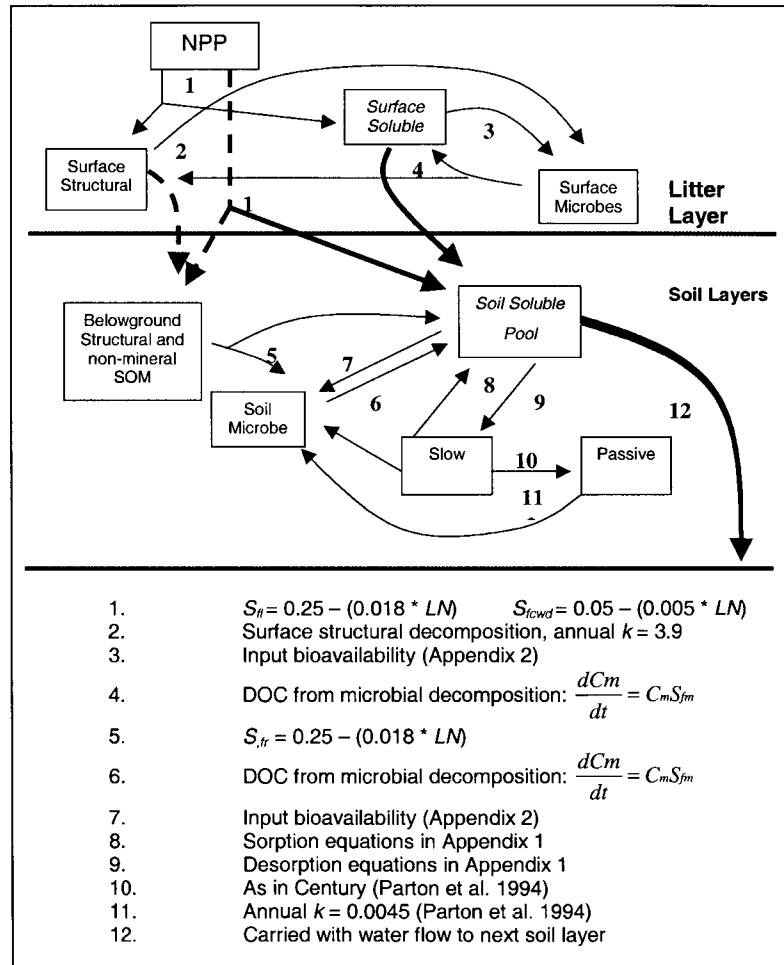Water fluxes in the soil are described by Richards Equation:

$$\frac{\partial\theta}{\partial t} = \frac{\partial}{\partial z}\left[k\left(\frac{\partial\theta}{\partial z}\frac{\partial\varphi}{\partial\theta} + 1\right)\right] \tag{5}$$

where k is the hydraulic conductivity and φ is the soil matrix potential. Boundary conditions are water inputs at the top of the soil column and drainage from the bottom. The hydraulic conductivity and soil matrix potential vary with volumetric water content (θ) and soil texture based on relationships developed by Clapp and Hornberger (1978) and Cosby et al. (1984). Thus, soil texture is an important input parameter set for TerraFlux (Appendix 2).

Plant-soil carbon transfers and soil organic carbon

The soil carbon pool structure of TerraFlux is similar to that of Century (Parton et al. 1994), but functionally important changes have been developed for our model. The equations governing carbon transfer between pools are given in Figure A3. A unique feature of TerraFlux is its emphasis on the flow and stabilization of dissolved organic carbon (DOC) and nutrients with soil depth. The classic "slow" and "passive" soil carbon pools as developed by Parton et al. (1987), Schimel et al. (1994), etc., and as experimentally tested by Trumbore (1993), Townsend et al. (1995), and others are used in TerraFlux. However, the movement of C between pools is governed by microbial activity and geochemical-hydrological transport controls, as discussed below.

As precipitation moves through plant canopies, it becomes significantly enriched in dissolved organic materials (Dalva & Moore 1991, Koprivnjak & Moore 1992). Therefore, dissolved organic carbon (DOC) enrichment of throughfall water is scaled from 0–150 mg DOC-CL^{-1} based on the effective canopy transport depth [= f(LAI, leaf angle distribution)]. The solubility of litter is an input variable in TerraFlux and is typically selected at 0.5 based on

1. $S_{fl}= 0.25 - (0.018 * LN)$ $S_{fcwd}= 0.05 - (0.005 * LN)$
2. Surface structural decomposition, annual $k = 3.9$
3. Input bioavailability (Appendix 2)
4. DOC from microbial decomposition: $\dfrac{dCm}{dt} = C_m S_{fm}$
5. $S_{,fr} = 0.25 - (0.018 * LN)$
6. DOC from microbial decomposition: $\dfrac{dCm}{dt} = C_m S_{fm}$
7. Input bioavailability (Appendix 2)
8. Sorption equations in Appendix 1
9. Desorption equations in Appendix 1
10. As in Century (Parton et al. 1994)
11. Annual $k = 0.0045$ (Parton et al. 1994)
12. Carried with water flow to next soil layer

A3. Litter layer and the top soil layer of the model; Carbon and nutrient transfers across these layers in TerraFlux. The litter and soil soluble (dissolved organics/inorganics) pools play a central role in calculating the transport of dissolved carbon and nutrients from layer to layer.

the review of Neff and Asner (2001) (Appendix 2); It is used to split the incoming litter C pool into structural and soluble fractions (Figure A3). This is analogous to the structural-metabolic division in the Century model which is based on laboratory assays linking hot water-soluble litter materials to litter lignin:N ratio (Parton et al. 1994):

$$S_{fl,fr} = 0.25 - (0.018 \bullet L : N) \tag{6}$$
$$S_{fcwd} = 0.05 - (0.005 \bullet L : N)$$

where S_{fl} is the soluble litter fraction, S_{fr} is the soluble fraction of roots and S_{fcwd} is the soluble fraction of the course woody debris at each time step, and L:N is the lignin to nitrogen ratio of the incoming litter.

Fluxes of DOC generally increase as water moves through the upper, organic rich horizons of the soil and then decrease with depth (Neff & Asner 2001). However, in virtually every soil with substantial clay content, DOC concentrations drop by 50–90% from the surface organic layers to sub-surface, mineral soils (McDowell & Wood 1984; Cronan & Aiken 1985; Dalva & Moore 1991; Koprivnjak & Moore 1992; Dosskey & Bertsch 1997). The model therefore reflects these numerous field studies indicating both physical and biological mechanisms controlling these transformations as outlined below.

Sorption isotherms

Sorption isotherms are commonly used to examine relationships between solution concentration and soil surface association. Because DOC moves in and out of solution continuously in soils, the Initial Mass (IM) isotherm best represents DOC sorption reactions (Nodvin et al. 1986; Kaiser et al. 1996):

$$RE = mX_i - b \tag{7}$$

where RE is the amount of DOC released into or removed from solution, m is the dimensionless regression (partition) coefficient, Xi is the initial concentration of DOC (mg g soil^{-1}), and b is the intercept (mg DOC released per gram soil if $Xi = 0$). Functionally, m and b can be viewed as measures of a soil's tendency to adsorb and release DOC. A comprehensive synthesis leading to the development of DOC sorption isotherms and a parameter (m, b) database within TerraFlux was given by Neff and Asner (2001). This database can be employed or the parameters can be developed for a particular site using a series of soil batch isotherm experiments. Ultimately, the sorption or desorption flux of DOC in each soil layer calculated as:

$$\frac{dC_{slow}}{dt} = m[DOC] - b[C_{slow}] - Fp - Fm \tag{8}$$

where m and b are the sorption and desorption parameters defined above, $dDOC/dt$ represents the flux of DOC to or from the actively sorbing C pool, Fp is the flow to the passive pool and Fm is the microbial decomposition of the slow C pool (Figure A3).

Microbial production of DOC

Neff and Asner (2001) discuss the direct links between microbial activity and DOC generation. The following equation represents the DOC generated during microbial decomposition:

$$\frac{dCm}{dt} = C_m S_{fm} \tag{9}$$

Cm is the turnover time of the microbial pool and S_{fm} is the total soluble fraction of microbial materal. For general, non site-specific simulations using TerraFlux, the soluble fraction of microbes is set to 50% for both surface (litter) and soil microbial populations (Figure A2). This fraction is roughly based on estimates of recovery rates for the soluble fraction of microbial biomass in chloroform fumigation, direct extraction measurements as well as an average protein content of bacteria, which we expect to be readily soluble (Beck et al. 1997).

Hydrologic control of DOC fluxes

Hydrologic conditions influence the leaching and apparent reactivity of dissolved organic material in terrestrial ecosystems. Within soils, factors such as hydraulic conductivity and capacity for bypass flow affect the concentrations and fluxes of inorganic elements in solution (e.g., Prendergast 1995), and it is likely that DOC behaves similarly (Radulivich et al. 1992). Weigand & Totshe (1998) provide strong evidence that water flow rate through soils affects the fate of DOC. Based on these results, the sorption affinity m is reduced by a modifier term (Hm) which scales with the rate of solution movement through the soil ($m = m - Hm$). This parameterization represents a kinetic aspect of the sorption reactions and a maximum flow rate induced variation in m of 20% in a soil with 100% clay content:

$$Hm = m^*0.2\left(\frac{v}{v_s}\right)\left(\frac{\%Clay}{100}\right) \tag{10}$$

where v is actual pore water velocity and v_s is the pore water velocity at saturated conditions.

In contrast, the desorption flux appears to be driven by concentration gradients and it increases with solution flow (Weigand & Tosche 1998). Thus, b is increased ($b = b + Hb$) by:

$$Hb = b^*0.2\left(\frac{v}{v_s}\right)\left(\frac{\%Clay}{100}\right) \tag{11}$$

As with the down-regulating Hm modifier, Hb scales with flow velocity and % clay content, but in contrast to flow effects on m, b is incremented by Hb to establish a flow-dependent desorption coefficient.

Soil nutrient cycling

Inorganic and organic forms of N, P, Ca, Mg and K can be simulated in TerraFlux, although to varying levels of mechanism and accuracy. Inorganic nutrients such as NH_4^+, NO_3^-, PO_4^-, and cations can enter the system via atmospheric deposition. Annual deposition rates (g m^{-2}) are specified as model input (Appendix 2), and are deposited into the surface soluble pool with rainfall events (c.f. Currie & Aber 1999). Once in the surface soluble pool – which is a microbe-available solution containing dissolved elements – nutrients can be immobilized during C decomposition or, when hydrological flow permits, nutrients can be transported into the soil column to the soil soluble pools. Rock-derived nutrients such as P, Mg, K, and Ca can also enter the soil soluble pool via weathering; The rate of input is given on an annual basis and is temporally partitioned with increased water flow 'events' through the soil.

Soil microbes preferentially draw (immobilize) nutrients from soil solution but also have access to nutrients derived from the turnover of slow and passive organic matter pools (Figure A2). Nutrient turnover from the slow and passive pools is modeled using first-order differential equations and the C:nutrient stoichiometry of the donor and receiver pools during decomposition (e.g., Parton et al. 1987, 1994).

Dissolved organic nutrients also enter the surface and soil soluble pools in stoichiometric balance with DOC (Neff et al. 2000). Soil microbes take up dissolved organic nutrients as they assimilate DOC, which is based on input parameters of bio-availability and microbial turnover (Neff & Asner 2001). At present, dissolved organic nutrients can be sorbed and desorbed within each soil layer only based on the sorption-desorption dynamics of DOC (described above). We recognize that the sorption dynamics of dissolved organic nutrients such as P may

not be represented well with this simple approach (e.g., Neff et al. 2000), and effort is currently underway to improve this formulation. Nonetheless, a general lack of data precludes another approach.

Inorganic nutrients can be sorbed onto the non-mineral SOM and mineral soil pools, or can be immobilized by soil microbes during C decomposition. Sorption and desorption affinities for any nutrient that is 'turned on' in the model must be provided as input. Since the sorption-desorption isotherms of NH_4^+, NO_3^-, PO_4^-, and cations vary widely with soil texture, mineralogy, pH, SOM content and other factors (e.g., Lopez-Hernandez & Burnham 1974), this approach severely limits the use of the model in multiple-nutrient mode for large regional or global applications. Therefore, in large-scale applications, most of these nutrients are turned off and only C and N are simulated. However, we contend that the ability to turn on various nutrients for site-level or purely theoretical analyses provides a means to test hypotheses regarding biological and geochemical controls over nutrient transport and stabilization as well as multiple nutrient controls on plant productivity. For any element simulated in TerraFlux, geochemical sorption competes directly with biological (microbial) immobilization; Analysis of this competition is an example of the usefulness of this multiple element approach.

In TerraFlux, cation and anion sorption isotherms vary with the molecule of interest and with soil properties, but are based on the modified Freundlich isotherm (e.g., Afif et al. 1995):

$$X = Ac^b t^d \tag{12}$$

where X is the amount of nutrient sorbed (mg nutrient/mg soil), c is the equilibrium concentration of the nutrient in solution (mg nutrient/L), t is time, and A, b, and d are fitting parameters derived by nutrient and soil type. Although the latter parameters are empirical, A represents the sorption affinity, and b and d effectively represent the fast and slow component of the reaction, respectively. Other isotherms can be readily incorporated into TerraFlux; The Langmuir isotherm has been extensively studied (e.g., Taylor et al. 1996). Here, we use the modified Freundlich isotherm for its simplicity and because the most common isotherm equations yield similar results (Mead 1981). In comparison to DOC isotherms, cations can readily sorb in soils with high cation exchange capacity (CEC) while anions sorb in soils with high anion exchange capacity (AEC). Therefore, the non-linear behavior of the Freundlich, Langmuir and other isotherms of this type is essential to simulate the sorption dynamics of inorganic nutrients in soil. Of all molecules simulated in TerraFlux, phosphate (PO_4^-) is the most difficult to employ due to the complicated fast and slow sorption reactions that are involved (Dzombak & Morel 1990). This impedes accurate simulation of the geochemical dynamics of P. While we recognize that no isotherm can easily account for the observed "slow component" of the sorption kinetics of a nutrient (e.g., Freese et al. 1995), we do favor the use of isotherms for a lack of a better approach.

Microbial immobilization of nutrients is a function of microbial stoichiometry, as in the Century model (Parton et al. 1987, 1994). Similarly, all dissolved organic and inorganic nutrients can be parameterized to stabilize in occluded forms based on a uni-directional first-order differential equation:

$$\frac{dP_{occ}}{dt} = \gamma X \tag{13}$$

where X is the amount of nutrient sorbed at time t, and γ is a parameter representing the occlusion rate constant.

Inorganic nutrient leaching

Similar to dissolved organic C and nutrients, inorganic forms of any simulated nutrient can be vertically transported through the soil. The factors that regulate these flows include water transport, microbial immobilization and mineralization, and the sorption/occlusion affinity of the soil. More specifically, the advective flux of inorganic nutrients is computed as:

$$F_i = C_{w,i} Q \qquad (14)$$

where $C_{w,i}$ is the aqueous concentration of inorganic nutrient i (kg m^{-3}) and Q is the bulk water flow (m^3 s^{-1}). Dispersion of soluble compounds is ignored. As discussed earlier, water flow through a layer is dependent upon water input and the hydrological parameters provided or estimated from soil texture (hydraulic conductivity, soil matrix potential). Microbial immobilization and mineralization of nutrients along the vertical soil pathway is a function of C:nutrient stoichiometry and C turnover (as in the Century model by Parton et al. (1987, 1994)). Sorption and desorption isotherms must be provided by soil layer in the model (Appendix 2).

Inorganic N transformations in soil

In each soil layer, mineralized nitrogen is empirically partitioned into NH_4^+ and NO_3^- forms. While we recognize that nitrification is a critically important process affecting sorption and leaching dynamics (as well as other processes such as N trace gas emissions), too little information exists to mechanistically represent the effects of nitrifying bacteria. Until we are able to take this important step, we use an input parameter to partition mineralized N into NH_4^+ and NO_3^- pools (Appendix 2).

Biological N fixation and inorganic N uptake

Biological nitrogen fixation (BNF) can represent an important flux of N into terrestrial ecosystems. In TerraFlux, BNF rates are empirically derived from its observed correlation with evapotranspiration by Cleveland et al. (1999), which was modified by Asner and Cleveland (*in review*) to account for the spatial density of nitrogen fixers at the ecosystem level as inferred from BNF analyses relative to plant N requirement. BNF-derived nitrogen enters the plant and is allocated evenly across foliage, roots, and wood depending upon carbon allocation requirement and C:N stoichiometry. This source of N is used by the plant prior to the uptake of inorganic N from soil soluble pools. If the combination of plant N resorption (discussed above) and BNF do not accommodate the estimated NPP at a given model time step, then the plant draws from soil inorganic N pools. In this case, the total inorganic N requirement is calculated, and vegetation takes up NH_4 and NO_3 in equal proportions from soil soluble pools. The total $NH_4^+ + NO_3^-$ taken from each soil layer is partitioning by the root distribution. If a particular soil layer cannot supply a sufficient amount of inorganic N, then other layers are drawn from in an iterative manner until total N requirement of the vegetation is met.

Balancing C and nutrient cycles

A unique feature of TerraFlux is that nutrient cycles are 'equilibrated' with estimates of NPP prior to starting a particular experiment. The approach is derived from the understanding that serious uncertainty in many of the processes represented in this (and other) biogeochemical

models makes it difficult to realistically model nutrient transfers in plants and soil. Given that biogeochemical processes within the plant-soil system have no particular beginning or end point (they are cycles), we strive to estimate NPP with as much accuracy or realism as is possible. From there, we can then equilibrate many processes to the 'known' NPP.

The equilibration is comprised of three distinct phases. First, time-series NPP is estimated from satellite LAI/fPAR, downwelling PAR, and hydrologic-energy balance modules as described above. These NPP estimates are then checked against either local data (if the model is running at a point scale) or against the *sim900* point database of field-measured NPP provided by Scurlock et al. (1999). We keyed this database, via geographic locational information, to a 1 km resolution global satellite map of vegetation type (Defries & Townshend 1995), then scaled the NPP point data to the vegetation cover estimates in the map. Finally, we smoothed the NPP map – hereafter called the "validation map". We iteratively recalculate the TerraFlux NPP estimates to best match the distribution of NPP in the validation map. This method is similar to that of Field et al. (1995). During the model spin up, the N stress factor (eq. 2) is fixed at 1.0 as the soil N pools are filled to a level that supports enough N mineralization for NPP (eq. 3).

The second phase in the equilibration involves the building up of carbon and nutrient pools. This is done in the same way that Century (Parton et al. 1994; Schimel et al. 1994) and similar models build model pools to quasi-equilibrium. During this phase, nutrients are added to soluble surface and soil pools to bring the model to an equilibrated state.

Finally, unresolved dependencies are rectified and the satellite-driven NPP is turned off. The most common unresolved dependency occurs when a nutrient is not built up sufficiently in the soluble pools to accommodate 'known' NPP. At this point, plant C:nutrient ratios, atmospheric deposition (for any nutrient), weathering (for rock-derived nutrients), or biological fixation (for nitrogen) can be adjusted, or NPP can be down-regulated until equilibration is achieved. In general, we down regulate NPP by as much as 5% and increase C:nutrient ratios up to 10–20% to accommodate a smaller NPP-driven uptake of soil inorganic nutrients. Thus, C:nutrient ratios are permitted to float by +/– 10–20% of their initial input value (Appendix 2). If these measures do not rectify the mismatch between NPP and nutrient availability, we can increase deposition, weathering inputs, and BNF where appropriate in 1% increments until NPP is satisfied. However, we have rarely encountered this situation. Once all cycles are balanced, the satellite-driven NPP is turned off, and NPP follows climate and nutrient controls in a similar manner as other non-satellite driven models.

Appendix 2. Base case input variables required for the TerraFlux model of humid tropical forests and semi-arid savannas. Representative data sources are given.

Input Variables	Lowland Tropical Evergreen Forest	Semi-arid grassland	Example Sources for Global/ General Analyses
Climate			
Surface Temperature	Figure 1a[+]	Figure 1d[+]	ECMWF (1998)
Precipitation	Figure 1b[+]	Figure 1e[+]	ECMWF (1998)
Cloud cover	Not shown	Not shown	ECMWF (1998)

Shortwave Radiation Down	Figure 1c[+]	Figure 1f[+]	ECMWF (1998)
Surface Pressure	Not shown	Not shown	ECMWF (1998)
Wind Speed	Not shown	Not shown	ECMWF (1998)
Vegetation			
Type	Evergreen Broadleaf	Tallgrass Priarie	Defries et al. (1995)
Percentage Canopy Cover	85–100%	50–100%	Defries et al. (1995)
Mean Canopy Height	30m	0.3m	Bonan (1996)
Leaf Angle Distribution	Uniform	Erectophile	Asner (1998)
Stem (wood) Area Index	0.5	0.0	Bonan (1996), Asner (1998)
Foliage			
Optical Properties	VIS:7%, NIR:44%	VIS:12%, NIR:38%	Asner et al. (1998a) and Asner (1998)
C:N$	30	49	Parton et al. (1994), Asner and Matson (*in prep.*)
C:P*	5000	480	Parton et al. (1994), Asner and Matson (*in prep.*)
C:Ca*	70	42	Asner and Matson (*in prep.*)
N Resorption	80%	90%	Vitousek (1982), Killingbeck (1996), Aerts (1996)
P Resorption*	95%	80%	Vitousek (1982), Killingbeck (1996)
Ca Resorption*	85%	80%	Vitousek (1982)
Wood			
Optical Properties	VIS:0.24, NIR:0.36	VIS:0.42, NIR:0.53[+]	Asner et al. (1998a) and Asner (1998)
C:N$	80	—	Parton et al. (1994)
C:P*	1500	—	Asner and Matson (*in prep.*)

C:Ca*	110	—	Asner and Matson (*in prep.*)
N Resorption	0%	—	Inferred from Gordon and Jackson (2000)
P Resorption*	0%	—	Inferred from Gordon and Jackson (2000)
Ca Resorption	0%	—	Inferred from Gordon and Jackson (2000)
Coarse/Fine Roots			
C:N$	70–90/40–50	70–90/40–50	Parton et al. (1994), Gordon and Jackson (2000)
C:P*	900–1000/475–525	900–1000/475–525	Parton et al. (1994), Gordon and Jackson (2000)
C:Ca*	100–150/80–100	100–150/80–100	Gordon and Jackson (2000)
N Resorption	0–5%	0–5%	Gordon and Jackson (2000)
P Resorption*	0–5%	0–5%	Gordon and Jackson (2000)
Ca Resorption*	0–5%	0–5%	Estimated from Vitousek (1982)
Distribution In Soil Profile	By biome	By biome	Jackson et al. (1996)
Coarse:Fine Root Ratio	9:1	1:20	Jackson et al. (1997)
Soils			
Physical			
Depth	> 10m	> 3m	Site specific
Texture (% sand,silt,clay)	30,10,60%	40,20,40%	Boutton et al. (1998), Silver et al. (1999)
Chemical			
Soil C:N#	10,10,15,10	10,10,20,10	Parton et al. (1994), Schimel et al. (1996)
Soil C:P#*	50,90,150,80	50,90,150,80	Parton et al. (1994)
Soil C:Ca#*	30,40,90,40	30,40,90,40	Insufficient data; Estimated between C:N and C:P values and supported by Staff and berg (1982)
DOC Sorption Affinity (m)	0.2–0.32	0.15–0.28	Neff and Asner (2001)
DOC Desorption	0.01–0.15	0.25–0.35	Neff and Asner (2001)

Affinity (b)			
DOC	40–60%	40–60%	Neff and Asner (2001)
Bioavailability			
DOC Solubility	30–60%	30–60%	Neff and Asner (2001)
DOC:DON	20–50	20–50	Neff et al. (2000)
DOC:DOP*	200–600	200–600	Neff et al. (2000)
DOC:DOCa*	0	0	Insufficient data; Turned off for these analyses
NH_4 Isotherms (A, b, d)	A: $2e10^{-8}$ b: 0.2 d: 0.0*	A: $5e10^{-3}$ b: 1.0 d: 0.0*	Hunt and Adamsen (1985), Matschonat and Matzner (1995)
NO_3 Isotherms (A, b, d)	A: $4e10^{-4}$ b: 0.8 d: 0.2*	A: $8e10^{-5}$ b: 0.5 d: 0.0*	Cahn et al. (1992); but there is generally insufficient data
PO_4 Isotherms (A, b, d)	A: $8e10^{-3}$ b: 0.2 d: 0.1*	A: $1e10^{-3}$ b: 0.1 d: 0.0*	Afif et al. (1995), Nakos (1987), Iniguez and Val (1984)
Ca Isotherms (A, b, d)	A: $2e10^{-3}$ b: 0.7 d: 0.1*	A: $1e10^{-3}$ b: 0.4 d: 0.1*	Marcano-Martinez and McBride (1989)
Occlusion Rate Const (γ)	10^{-5}	10^{-10}	Estimated from Hillel (1998)
NH_4:NO_3	1:10	1:2	e.g., Blair (1997), Vitousek and Matson (1988)
Partitioning			

* = optional parameter
LUT = look up table;
VIS = visible wavelengths (400–700nm); NIR = near-IR wavelengths (700–2500nm); + = canopy litter (senescent grass)
\# = order is soluble, microbial, slow, passive
$ = C:nutrient ratios can float by +/– 10% of input value

References

Aber JD & Driscoll CT (1997) Effects of land use, climate variation, and N deposition of N cycling and C storage in northern hardwood forests. Global Biogeochemical Cycles 11: 639–648

Aber JD, McDowell W, Nadelhoffer K, Magill A, Berntson G, Kamakea M, McNulty S, Currie W, Rustad L & Fernandez I (1998) Nitrogen saturation in temperate forest ecosystems: Hypotheses revisited. BioScience 48: 921–934

Aber J, Nadelhoffer KJ, Steudler P & Melillo JM (1989) Nitrogen saturation in northern forest ecosystems. BioScience 39: 378–386

Abrahams AD, Parsons AJ & Wainwright J (1995) Effects of vegetation change on interrill runoff and erosion, Walnut Gulch, southern Arizona. Geomorphology 13: 37–48

Aerts R (1996) Nutrient resorption from senescing leaves of perennials: are there general patterns? Journal of Ecology 84: 597–609

Afif E, Barron V & Torrent J (1995) Organic matter delays but does not prevent phosphate sorption by cerrado soils from Brazil. Soil Science 159: 207–211

Agren G & Bosatta E (1988) Nitrogen saturation of terrestrial ecosystems. Environmental Pollution 54: 185–197

Arya SP (1988) Introduction to Micrometeorology. Academic Press, San Diego, CA

Asner GP (1998) Biophysical and biochemical sources of variability in canopy reflectance. Remote Sensing of Environ. 64: 134–153

Asner GP (2000) A hyperspectral photon transport system for simulating imaging spectrometer observations of terrestrial ecosystems. Proceedings of the Airborne Earth Science Workshop, NASA JPL Technical Memo 99-17

Asner GP, Bateson CA, Privette JL, Saleous N El & Wessman CA (1998a) Estimating vegetation structural effects on carbon uptake using satellite data fusion and inverse modeling. Journal of Geophysical Research 103: 28, 839–828, 853

Asner GP & Cleveland CC. Biological nitrogen fixation in terrestrial ecosystems: new estimates based on modeled constraints. Global Biogeochemical Cycles (in review)

Asner GP & Matson PA (in prep.) Concentrations of N, P and base cations in live foliage and woody material: a global synthesis

Asner GP & Wessman CA (1997) Scaling PAR absorption from the leaf to landscape level in spatially heterogeneous ecosystems. Ecological Modelling 103: 81–97

Asner GP, Wessman CA, Schimel DS & Archer S (1998b) Variability in leaf and litter optical properties: implications for BRDF model inversions using AVHRR, MODIS and MISR. Remote Sensing of Environ. 63: 200–215

Asner GP, Seastedt TR & Townsend AR (1997) The decoupling of terrestrial carbon and nitrogen cycles. BioScience 47(4): 226–234

Bach LB, Wierenga PJ & Ward TJ (1986) Estimation of the Philip infiltration parameters from rainfall simulation data. Soil Science Society of America J 50: 1319–1323

Beck T, Joergensen RF & Sheu S (1997) An inter-laboratory comparison of ten different ways of measuring soil microbial biomass carbon. Soil Biology and Biochemistry 29: 1023–1032

Berendse F, Aerts R & Bobbink R (1993) Atmospheric nitrogen deposition and its impact on terrestrial ecosystems. In Odam CVP (Ed.) Landscape Ecology of a Stressed Environment (pp 104–121). Chapman and Hall, London

Binkley D & Hogberg P (1997) Does atmospheric deposition of nitrogen threaten Swedish forests? Forest Ecology and Management 92: 119–152

Blair JM (1997) Fire, N availability and plant response to grasslands: a test of the transient maxima hypothesis. Ecology 78: 2359–2368

Bonan GB (1994) Comparison of two land surface process models using prescribed forcings. J Geophysical Research 99: 25, 803–25, 818

Bonan GB (1996) A land surface model (LSM Version 1.0) for ecological, hydrological and atmospheric studies: Technical description and user's guide. NCAR Technical Note TN-417+STR, National Center for Atmospheric Research, Boulder, CO

Boutton TW, Archer S, Midwood AJ, Zitzer SF & Bol R (1998) d13C values of soil organic carbon and their use in documenting vegetation change in a subtropical savanna ecosystem. Geoderma 85: 5–41

Brutsaert W (1982) Evaporation into the atmosphere: Theory, history and applications. D Reidel Publishing Co., Dordrecht

Cahn MD, Bouldin DR & Cravo MS (1992) Nitrate sorption in the profile of an acid soil. Plant and Soil 143: 179–183

Chameides WL, Kasibhatla PS, Yeinger J & Levy H II (1994) Growth of continental-scale metro-agro-plexes, regional ozone pollution, and world food production. Science 264: 74–77

Clapp RB & Hornberger GM (1978) Empirical equations for some soil hydraulic properties. Water Resources Research 14: 601–604

Cleveland CC, townsend AR, Schimel DS, Fisher H, Howarth RW, Hedin LO, Perakis SS, Latty EF, Von Fischer JC, Elseroad A & Wasson MF (1999) Global patterns of terrestrial biological nitrogen (N2) fixation in natural ecosystems. Global Biogeochemical Cycles 13: 623–645

Cosby BJ, Hornberger GM, Clapp RB & Ginn TR (1984) A statistical exploration of the relationships of soil moisture characteristics to the physical properties of soils. Water Resources Research 20: 682–690

Cromack K (1973) Litter production and decomposition in a mixed hardwood watershed and a white pine watershed at Coweeta Hydrologic Laboratory, North Carolina. Ph.D. Dissertation, University of Georgia, Athens, GA.

Cronan CS & Aiken GR (1985) Chemistry and transport of soluble humic substances in forested watersheds of the Adirondack Park, New York. Geochimica et Cosmochimica Acta 49: 1697–1706

Cuevas E & Medina E (1988) Nutrient dynamics within Amazonian forests. II. Fine root growth, nutrient availability, and leaf litter decomposition. Oecologia 76: 222–235

Currie W, Aber JD, McDowell WH, Boone RD & Magill AH (1996) Vertical transport of dissolved organic C and N under long-term N amendments in pine and hardwood forests. Biogeochemistry 35: 471–505

Currie WS & Aber JD (1997) Modeling leaching as a decompostion process in humid montane forests. Ecology 78: 1844–1860

Currie W & Nadelhoffer K (1999) Dynamic redistribution of isotopically labeled cohorts of nitrogen inputs in two temperate forests. Ecosystems 2: 4–18

Dalva M & Moore TR (1991) Sources and sinks of dissolved organic carbon in a forested swamp catchment. Biogeochemistry 15: 1–19

DeFries RS, Field CB , Fung I, Justice CO, Los S, Matson PA, Matthews E, Mooney HA, Potter CS, Prentice K, Sellers PJ, Townshend JR, Tucker CJ, Ustin SL & Vitousek PM (1995) Mapping the land surface for global atmosphere-biosphere models: Toward continuous distributions of vegetation's functional properties. J Geophysical Research 100: 20, 867–20, 883

Defries RS & Townshend JRG (1995) NDVI-derived land cover classifications at a global scale. International Journal of Remote Sensing 15: 3567–3586

Dosskey MG & Bertsch PM (1997) Transport of dissolved organic matter through a sandy forest soil. Soil Science Society of America J 61: 920–927

Dzombak DA & Morel FMM (1990) Surface Complexation Modeling. John Wiley & Sons, New York, NY

ECMWF (1998) Globally gridded climate data. European Centre for Medium-Range Weather Forecasts, http://www.ecmwf.int.

Emmett BA, Brittain A, Hughes S, Gorres J, Kennedy V, Norris D, Rafarel R, Reynolds B & Stevens PA (1995) Nitrogen additions at Aber forest, Wales. I. Response of throughfall and soil water chemistry. Forest Ecology and Management 71: 45–60

Fenn ME, Poth MA, Aber JD, Baron JS, Bormann BT, Johnson DW, Lemly AD, McNulty SG, Ryan DF & Stottlemyer R (1998) Nitrogen excess in North American ecosystems: predisposing factors, ecosystem responses, and management strategies. Ecological Applications 8: 706–733

Field CB, Randerson JT & Malmstrom CM (1995) Global net primary production: combining ecology and remote sensing. Remote Sensing of Environment 51: 74–88

Freese D, van Riemsdijk WH & SEATM van der Zee (1995) Modeling phosphate-sorption kinetics in acid soils. European J Soil Science 46: 239–245

Friedlingstein P, Joel G, Field CB & Fung IY (1999) Towards an allocation scheme for global terrestrial carbon models. Global Change Biology 5: 755–770

Galloway J, Levy II H & Kasibhatla PS (1994) Year 2020: consequences of population growth and development on deposition of oxidized nitrogen. Ambio 23: 120–123

Galloway JN, Schlesinger WH, Levy II H , Michaels A & Schnoor JL (1995). Nitrogen fixation: anthropogenic enhancement-environmental response. Global Biogeochemical Cycles 9: 235–252

Gordon WS & Jackson RB (2000) Nutrient concentrations in fine roots. Ecology 81: 275–280

Hall SJ & Matson PA (1999) Nitrogen oxide emissions after nitrogen additions in tropical forests. Nature 400: 152–155

Hillel D (1998) Environmental Soil Physics. Academic Press, San Diego, CA

Holland EA, Braswell BH, Lamarque J-F, Townsend AR, Sulzman J, Muller J-F, Dentener FJ, Brasseur G, Levy H, Penner JE & Roelofs G-J (1997) Variations in the predicted spatial distribution of atmospheric nitrogen deposition and their impact on carbon uptake by terrestrial ecosystems. J Geophysical Research 102: 15, 849–15, 866

Holland EA, Dentener FJ, Braswell BH & Sulzman JM (1999) Contemporary and pre-industrial global reactive nitrogen budgets. Biogeochemistry 46: 7–43

Howarth RW, Billen G & Zhao-Liang Z (1996) Regional nitrogen budgets and riverine N&P fluxes for the drainages to the North Atlantic Ocean: natural and human influences. Biogeochemistry 35: 181–226

Hudson R, Gherini SA & Goldstein RA (1994) Modeling the global carbon cycle: nitrogen fertilization of the terrestrial biosphere and the missing CO2 sink. Global Biogeochemical Cycles 8: 307–333

Hunt HW & Adamsen FJ (1985) Empirical representation of ammonium adsorption in two soils. Soil Science 139: 205–211

Iniguez J & Val RM (1984) Evaluation of phosphorus sorption by an allophonic soil. Geoderma 33: 119–134

Jackson RB, Mooney HA & Schulze ED (1997) A global budget for fine root biomass, surface area, and nutrient contents. Proceedings of the National Academy of Sciences 94: 7362–7366

Kaiser K, Guggenberger G & Zech W (1996) Sorption of DOM and DOM fractions to forest soils. Geoderma 74: 281–303

Killingbeck KT (1996) Nutrients in senesced leaves: keys to the search for potential resorption and resorption efficiency. Ecology 77: 1716–1728

Koprivnjak JF & Moore TR (1992) Sources, sinks and fluxes of dissolved organic carbon in subarctic fen catchments. Arctic and Alpine Research 24: 204–219

Lajtha K & Bloomer SH (1988) Factors affecting phosphate sorption and phosphate retention in a desert ecosystem. Soil Science 146: 160–167

Lelieveld J & Dentener FJ (2000) What controls tropospheric ozone? J Geophysical Research 105: 3531–3543

Likens GE, Driscoll CT & Buso DC (1996) Long-term effects of acid rain: response and recovery of a forest ecosystem. Science 272: 244–246

Logan J (1983) Nitrogen oxides in the troposphere: global and regional budgets. J Geophysical Research 88: 10, 785–10, 807

Lopez-Hernandez ID & Burnham CP (1974) The covariance of phosphate sorption with other soil properties in some British and tropical soils. J Soil Science 25: 196–205

Magill AH, Aber JD, Hendricks JJ, Bowden RD, Melillo JM & Steudler PA (1997) Biogeochemical response of forest ecosystems to simulated chronic nitrogen deposition. Ecological Applications 7: 402–415

Marcano-Martinez E & McBride MB (1989) Calcium and sulfate retention by two oxisols of the Brazilian Cerrado. Soil Science Society of America J 53: 63–69

Matschonat G & Matzner E (1995) Quantification of ammonium sorption in acid forest soils by sorption isotherms. Plant and Soil 168: 95–101

Matson P, McDowell W, Townsend A & Vitousek P (1999) The globalization of N deposition: ecosystem consequences in tropical environments. Biogeochemistry 46: 67–83

McDowell WH & Wood T (1984) Podzolization: soil processes control dissolved organic carbon concentrations in stream water. Soil Science 137: 23–32

McLendon T & Redente EF (1992) Effects of nitrogen limitation on species replacement dynamics during early succession during early succession on a semi-arid sagebrush site. Oecologia 91: 312–317.

Mead JA (1981) A comparison of the Langmuir, Freundlich and Temkin equations to describe phosphate adsorption properties of soils. Australian J Soil Research 19: 333–342

Medina E & Silva JF (1990) Savannas of northern South America: a steady state regulated by water-fire interactions on a background of low nutrient availability. J Biogeograhy 17: 403–413

Milchunas DG & Lauenroth WK (1993) Quantitative effects of grazing on vegetation and soils over a global range of environments. Ecological Monographs 63: 327–366

Nadelhoffer KJ, Emmett BA, Gundersen P, Kjonass OJ, Koopmans CJ, Schleppi P, Tietma A & Wright RF (1999) Nitrogen deposition makes a minor contribution to carbon sequestration in temperate forests. Nature 398: 145–148

Nakos G (1987) Phosphorus adsorption by forest soils. Communications in Soil Science and Plant Analysis 18: 279–286

Neff JC & Asner GP (2001) Dissolved organic carbon in terrestrial ecosystems: synthesis and a model. Ecosystems 4: 29–48

Neff JC, Hobbie S & Vitousek PM (2000) Controls over the production and stoichiometry of dissolved organic carbon, nitrogen and phosphorus in tropical soils. Biogeochemistry 51: 283–302

Nishita H & Haug RM (1973) Distribution of different forms of nitrogen in some desert soils. Soil Science 116: 51–58.

Nodvin SC, Driscoll CT & Likens GE (1986) Simple partitioning of anions and dissolved organic carbon in a forest soil. Soil Science 142: 27–35

O'Connor TG (1994) Composition and population responses of an African savanna grassland to rainfall and grazing. J Applied Ecology 31: 155–171

Parton WJ, Ojima DS, Cole CV & Schimel DS (1994) A general model for soil organic matter dynamics: sensitivity to litter chemistry, texture, and management. Pages 147–167 in Quantitative Modeling of Soil Forming Processes. Soil Science Society of America, Madison, WI

Parton WJ, Schimel DS, Cole CV & Ojima DS (1987) Analysis of factors controlling soil organic matter levels in Great Plains grasslands. Soil Science Society of America J 51: 1173–1179

Paul EA & Clark FE (1996) Soil Microbiology and Biochemistry. Academic Press, San Diego

Peterson B & Melillo JM (1985) The potential storage of carbon caused by eutrophication of the biosphere. Tellus 37B: 117–127

Potter CS, Randerson JT, Field CB, Matson PA, Vitousek PM, Mooney HA & Klooster SA (1993) Terrestrial ecosystem production: a process model based on global satellite and surface data. Global Biogeochemical Cycles 7: 811–841

Prendergast JB (1995) Soil water bypass and solute transport under irrigated pasture. Soil Science Society of America J 59: 1531–1539

Radulovich R, Sollins P, Baveye P & Solorzano E (1992) Bypass water flow through unsaturated microaggregated tropical soils. Soil Science Society of America J 56: 721–726

Randerson JT, Thompson MV, Fung IY, Conway T & Field CB (1997) The contribution of terrestrial sources and sinks to trends in the seasonal cycle of atmospheric carbon dioxide. Global Biogeochemical Cycles 11: 535–560

Running SW, Loveland TR & Pierce LL (1994) A vegetation classification logic based on remote sensing for use in general biogeochemical models. Ambio 23: 77–81

Schimel DS, Braswell BH, Holland EA, McKeown R, Ojima DS, Painter TH, Parton WJ & Townsend AR (1994) Climatic, edaphic, and biotic controls over storage and turnover of carbon in soils. Global Biogeochemical Cycles 8: 279–293

Schindler D & Bayley S (1993) The biosphere as an increasing sink for atmospheric carbon: estimates from increased nitrogen deposition. Global Biogeochemical Cycles 7: 717–733

Schlesinger W, Abrahams AD, Parsons AJ & Wainwright J (1999) Nutrient losses in runoff from grassland and shrubland habitats in Southern New Mexico: I. Rainfall simulation experiments. Biogeochemistry 45: 21–34

Schlesinger W, Ward TJ & Anderson J (2000) Nutrient losses in runoff from grassland and shrubland habitats in Southern New Mexico: II. Field plots. Biogeochemistry 49: 69–86

Scurlock JMO, Cramer W & Prince SD (1999) Terrestrial NPP: Towards a consistent dataset for global model evaluation. Ecological Applications 9: 913–919

Seely, B & Lajtha K (1997) Application of a ^{15}N tracer to simulate and track the fate of atmospherically deposited N in the coastal forests of the Waquoit Bay Watershed, Cape Cod, Massachusetts. Oecologia 112: 393–402

Smil V (1991). Population growth and nitrogen: an exploration of a critical existential link. Populations and Development Review 17: 569–601

Staaf H & Berg B (1982) Accumulation and release of plant nutrients in a scots pine forest. Canadian J Botany 60: 1561–1568

Stoddard JL, Jeffries DS, Lukewille A, Clair TA, Dillon PJ, Driscoll CT, Forsius M & Johannessen M (1999) Regional trends in aquatic recovery from acidification in North America and Europe. Nature 401: 575–578

Taylor RW, Bleam WF & Tu SI (1996) On the Langmuir phosphate adsorption maximum. Communications in Soil Science and Plant Analysis 27: 2713–2722

Tietema A, Beier C, de Visser PH, Emmett BA, Gunderson P, Kjonaas OJ & Koopmans CJ (1997). Nitrate leaching in coniferous forest ecosystems: The European field-scale manipulation experiments NITREX and EXMAN. Global Biogeochemical Cycles 11: 617–626

Townsend AR, Vitousek PM & Trumbore SE (1995) Soil organic matter dynamics along gradients in temperature and land use on the island of Hawaii. Ecology 76: 721–733

Townsend AR, Braswell BH, Holland EA & Penner JE (1996) Spatial and temporal patterns in terrestrial carbon storage due to deposition of fossil fuel nitrogen. Ecological Applications 6: 806–814

Trumbore S (1993) Comparison of carbon dynamics in tropical and temperate soils using radiocarbon measurements. Global Biogeochemical Cycles 7: 275–290

Vitousek PM (1982) Nutrient cycling and nutrient use efficiency. American Naturalist 119: 553–572

Vitousek PM (1984) Litterfall, nutrient cycling and nutrient limitation in tropical forests. Ecology 65: 285–298

Vitousek PM & Field CB (1999) Ecosystem constraints to symbiotic nitrogen fixers: a simple model and its implications. Biogeochemistry 46: 179–202

Vitousek PM & Sanford R (1986) Nutrient cycling in moist tropical forests. Annual Reviews Ecology Systematics 17: 137–167

Vitousek P & Matson PA (1988) Nitrogen transformation in tropical forest soils. Soil Biology and Biochemistry 20: 361–367

Vitousek PM & Howarth RW (1991) Nitrogen limitation on land and in the sea: How can it occur? Biogeochemistry 13: 87–115

Vitousek PM, Aber JD, Howarth RW, Likens GE, Matson PA, Schindler DW, Schlesinger WH & Tilman GD (1997) Human alteration of the global nitrogen cycle: Sources and consequences. Ecological Applications 7: 737–750

Weigand H & Totsche KU (1998) Flow and reactivity effects on dissolved organic matter transport in soil columns. Soil Science Society of America Journal 62: 1268–1274

Wright R & N Van Breemen (1995) The NITREX project: an introduction. Forest Ecology and Managment 71: 1-6